Master's Thesis

Radio Resource Management for M2M Communication in LTE

By

Wang Fu

Department of Electrical and Information Technology
Faculty of Engineering, LTH, Lund University
SE-221 00 Lund, Sweden

Abstract

The purpose of this study is to investigate the behaviors of different link adaptation designs with signaling reduction in random access procedure with small infrequent data transfers for M2M traffic in LTE. Signaling reduction with efficient RRM is an aggressive optimization for such small data transfers to decrease the device energy consumption as well as to mitigate the high radio resource utilization issues.

Simulations have been run to illustrate how different link adaptation designs affect the radio resource utilization as well as to illustrate the behavior of device energy consumption for different models, based on whether or not discontinuous reception is used. Thirdly, the interaction between delay and device energy consumption is analyzed. Finally, the quality of the network service illustrated with the number of failure users is given.

The results show that signaling reduction with efficient RRM can potentially give good performance, as long as the data transfers are small and infrequent.

Acknowledgments

This Master's thesis would not exist without the support and guidance of Buon Kiong Lau in LTH, Lund University, Lund, as well as Erik Eriksson and Gunnar Bark in Ericsson Research, Ericsson AB, Linköping. They patiently helped and guided me a lot.

I would also like to give my thanks to Vanja Plicanic for her guidance, and for involving me in her project in Corporate Technology Office, Sony Ericsson Mobile Communications AB, Lund.

Many thanks to my family and friends for their love, patience and help.

Wang Fu

Table of Contents

Abstract 2

Acknowledgments 3

Table of Contents 4

1 Introduction 6

2 Problem formulation 12

2.1 Normal Scheme without Release Signaling 12

2.2 Static MCS Design 13

2.3 Dynamic MCS Design 14

2.4 Outer Loop MCS Design 15

2.5 Data Transfer Buffer Estimation Design 16

3 Simulation Setup 18

3.1 Simulation Scenarios 18

3.2 Radio Resource Utilization 19

3.3 Device Energy Consumption 19

3.3.1 Model Structure 19

3.3.2 Fine Clock 22

3.3.3 Receiver RF 22

3.3.4 Receiver Baseband 22

3.3.5 Power Amplifier (PA) 23

3.3.6 Transmitter RF 23

3.3.7 Transmitter Baseband 23

3.3.8 Model Parameters 23

3.4 Failure Users 24

3.5 Delay 24

4 Simulation Results 25

4.1 Radio Resource Utilization 25

4.1.1 Normal scheme without release signaling Case 1 25

4.1.2 Normal scheme without release signaling Case 3 27

4.1.3 Static MCS design Case 1 28

4.1.4 Static MCS design Case 3 29

4.1.5 Dynamic MCS design Case 1 30

4.1.6 Dynamic MCS design Case 3 32

4.1.7 Outer loop MCS design Case 1 33

4.1.8 Outer loop MCS design Case 3 34

4.1.9 Data transfer buffer estimation design Case 1 35

4.1.10 Data transfer buffer estimation design Case 3 36

4.2 Device Energy Consumption 38

4.2.1 Normal scheme without release signaling Case 1 38

4.2.2 Normal scheme without release signaling Case 3 40
4.2.3 Static MCS design Case 1 42
4.2.4 Static MCS design Case 3 45
4.2.5 Dynamic MCS design Case 1 47
4.2.6 Dynamic MCS design Case 3 49
4.2.7 Outer loop MCS design Case 1 51
4.2.8 Outer loop MCS design Case 3 53
4.2.9 Data transfer buffer estimation Case 1 55
4.2.10 Data transfer buffer estimation Case 3 57
4.3 Failure Users 59
4.3.1 Normal scheme without release signaling Case 1 59
4.3.2 Normal scheme without release signaling Case 3 59
4.3.3 Static MCS design Case 1 60
4.3.4 Static MCS design Case 3 61
4.3.5 Dynamic MCS design Case 1 61
4.3.6 Dynamic MCS design Case 3 62
4.3.7 Outer loop MCS design Case 1 62
4.3.8 Outer loop MCS design Case 3 63
4.3.9 Data transfer buffer estimation Case 1 63
4.3.10 Outer loop MCS design Case 3 64
4.4 Delay 64
4.4.1 Normal scheme without release signaling Case 1 65
4.4.2 Normal scheme without release signaling Case 3 65
4.4.3 Static MCS design Case 1 66
4.4.4 Static MCS design Case 3 66
4.4.5 Dynamic MCS design Case 1 67
4.4.6 Dynamic MCS design Case 3 67
4.4.7 Outer loop MCS design Case 1 68
4.4.8 Outer loop MCS design Case 3 68
4.4.9 Data transfer buffer estimation design Case 1 69
4.4.10 Data transfer buffer estimation design Case 3 69
5 Discussion 70
6 Conclusion 72
7 Items for future study 73
List of Acronyms 75
A.1 Effects of the setting of parameters in the outer loop MCS design 76
A.2 Energy consumption of each component in the different designs 79

CHAPTER 1

1 Introduction

Long Term Evolution (LTE) [1] was first deployed in Sweden in December, 2009. Since then, it has been experiencing a steady growth worldwide. More and more devices are now being added into LTE networks, including those used for machine-to-machine (M2M) communications. In fact, M2M traffic is expected to become an important part of LTE traffic. For example, a lot of sensors will use LTE networks to communicate with one another. Hence, it is a hot research topic nowadays to investigate how to manage these devices to fulfill their requirements, such as long battery life, less radio resource usage and shorter delay.

The purpose of this study is to show the advantages of efficient radio resource management (RRM) with signaling reduction for LTE M2M traffic in terms of more efficient radio resource usage, lower device energy consumption, good quality of network and shorter delay. This study requires good background knowledge of physical layer theory [2], RRM [3], scheduling and link adaptation [4], [5], Layer 1 and Layer 2 signaling [6], [7], random access procedures and connection setup procedures [1].

Some relevant technical papers of 3GPP technologies had been reviewed. For example, in [8], an energy-efficient link adaptation technique was investigated under the optimal conditions for efficient energy transmission, which occur over resources experiencing different channel conditions and algorithms developed, in order to acquire globally optimal solution. Simulation results on energy utilization provided indicate that there is at least 15% improvement if frequency selectivity is exploited [8]. However, in this thesis work, a different model is used for M2M communications with signaling reduction, and different link adaptation designs based on more analytical approaches are considered.

The impact of discontinuous reception (DRX) inactivity timer on power consumption of a mobile station was studied in [9], where analytic models were developed to investigate the power consumption with different types of traffic, for example bursty or streaming traffic [9]. One limitation of this

study is that it was done using 3G traffic model and real LTE traffic was not taken into account.

Another work [10] indicates that short DRX with inactivity timer can acquire a gain of 0-3 times over long DRX with the use of just an inactivity timer for bursty traffic. The work evaluated different performance criteria, such as device energy consumption, user capacity and quality of network based on its power model, which only considers the device energy consumption related to RF modem [10]. In contrast, in this thesis work, the exact value of energy consumption on each component in the power model can be determined with perfect DRX and without DRX. Moreover, this thesis also considers strict delay performance.

In summary, the main highlight of this thesis work as compared to earlier studies is to focus on optimized link adaptation designs with signaling reduction in LTE M2M scenarios and taking into account more analytical approaches.

As shown in Fig. 1, with small data transfers, a high proportion of the whole signaling steps are taken by a queue of RRC connection steps before uplink (UL) data transfers based on the LTE scheme [11]. This high proportion increases with fewer UL data transfers and decreases with reducing RRC connection steps. This high proportion could lead to high radio resource utilization and high terminal power consumption.

The idea is that the random access procedure should attempt to reduce the signaling steps when there is a small data transfer; meaning that those scheduled steps before the small data transfer are more likely to be simplified. However, it may lead to unsuccessful or inefficient data transfer due to poor link adaptation caused by insufficient signaling steps, for example if there is no Channel Quality Information (CQI) or data transfer buffer status report. Hence, a new scheme based on signaling reduction is needed. This is the motivation behind the link adaptation design in this thesis: since the signaling steps will be reduced, they will thus need to be scheduled by a new scheme, which will require some optimization.

As shown in Fig. 2 and Fig. 3, the signaling steps are drastically reduced, especially in the 4-way scheme. The scheme may make small data transfer successful even if there is no CQI or data transfer buffer status report. The reason for this is that as the data transfer involves a small packet size, the link adaptation will likely be designed to estimate proper Modulation and Coding Scheme (MCS) value or data transfer buffer size in the situation where E-UTRAN NodeB (eNB) could use special algorithm which, for

example, combines link adaptation with Random Access Channel (RACH) preamble sequence number to give a better scheme to estimate the status of the users who do not report channel quality or data transfer buffer size.

To help optimize the signaling reduction scheme while maintaining a satisfactory Quality of Service (QoS), several link adaptation designs are introduced. The basic concept is that these designs that are based on signaling reduction should make the RRM efficient. This means that if the design has better performance in criteria such as radio resource utilization, device energy consumption, failure users and delay, there will be an efficient RRM under these designs.

Also, to allow for further optimization of signaling reduction scheme under these designs, it is possible to have different settings of parameters specific to each design. For example, an aggressive setting may lead to a good performance on radio resource utilization but more failure users in the network, whereas a robust setting may have an opposite behavior.

For each link adaptation design used in this thesis, balancing of the aggressive/robust tradeoff is needed. This balance could be determined through verifying the performance of varying settings of parameters. This performance verification is made in terms of radio resource utilization, device energy consumption, number of failure users and delay.

Furthermore, in this thesis the performance of radio resource utilization is determined by the average Physical Uplink Shared Channel (PUSCH) usage, 95^{th} percentile PUSCH usage and average Physical Downlink Shared Channel (PDSCH) usage per User Equipment (UE). Effect on device energy consumption is analyzed via calculating average and 95^{th} percentile energy consumption per UE during the delay with perfect DRX and without DRX. There will be failure user(s) if the number of retransmission attempts on data transfer is larger than the defined maximum value. Delay is determined by the period that the random access procedure and the UL data transfer last.

Note the difference between signaling reduction with small infrequent data transfers and large data transfers: Even though there is shortage of CQI report or data transfer buffer size report, signaling reduction in random access procedure could make sure that small infrequent data transfers can be achieved if it is optimized by link adaptation design. For example, via statistics used in this thesis, the MCS value or data transfer buffer size could be assigned successfully. But for large data transfers, the signaling reduction would fail in estimating these parameters since there are more

attempts on data transfers during which the channel varies a lot. Thus, this thesis research is based on small infrequent UL data transfers that are common to some sensor devices, using the 4-way scheme in random access procedure.

To understand how link adaptation designs could be used to optimize signaling reduction scheme, several designs are introduced and studied in this thesis. These designs are named static MCS design, dynamic MCS design, outer loop MCS design and data transfer buffer estimation design. For each design, the aggressive method and robust method are given and simulated via varying settings of a specific parameter, as illustrated in Table 1. As a comparison between the LTE normal scheme and the signaling reduction scheme, a study case with signaling reduction in releasing signaling instead of random access procedure is also introduced and analyzed.

In Chapters 2 and 3, the problem formulation and the simulation setup are described. In Chapter 4, simulation results are presented. Chapter 5 gives the discussion and Chapter 6 gives the conclusion of the thesis work. Finally, Chapter 7 provides some suggestions future work.

TABLE 1. DESCRIPTION ON SETTINGS OF PARAMETERS UNDER EACH LINK ADAPTATION DESIGN.

Number	Design name	Description on setting of parameters
1	Static MCS design	Fixed MCS value
2	Dynamic MCS design	Relationship between SINR and RACH preamble sequence number
3	Outer loop MCS design	Statistic method used
4	Data transfer buffer estimation design	Relationship between buffer size assigned and RACH preamble sequence number

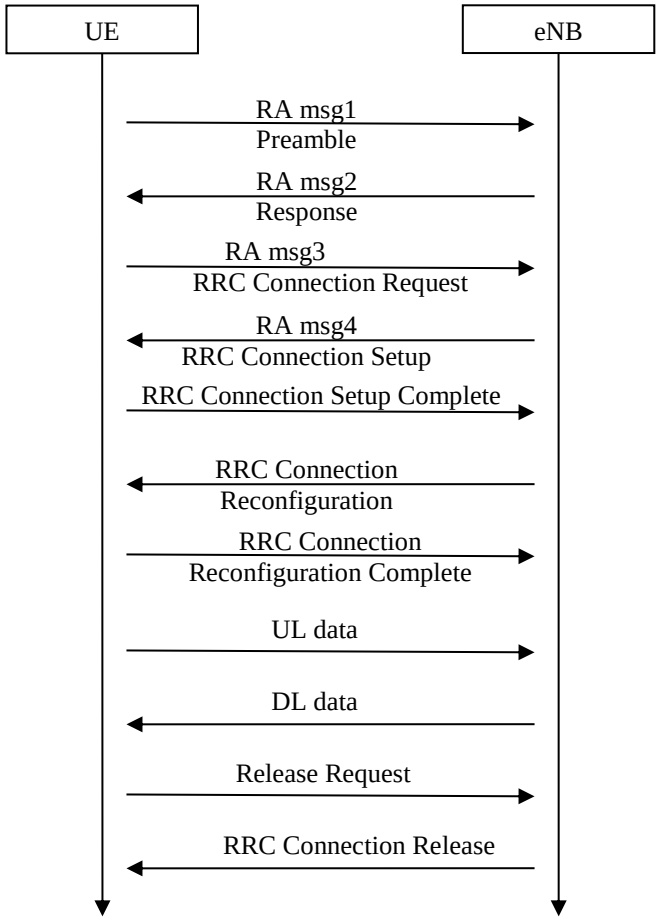

Fig. 1. Signaling steps between eNB and UE based on LTE scheme

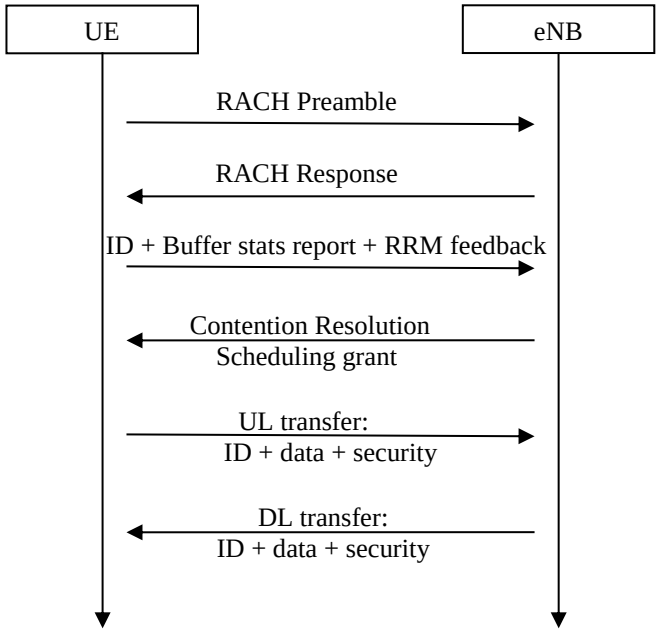

Fig. 2. Signaling reduction which is “6-way scheme”

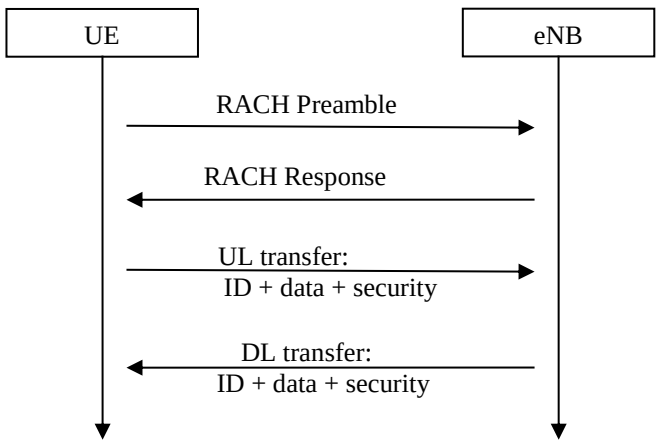

Fig. 3. Signaling reduction which is “4-way scheme”

CHAPTER 2

2 Problem formulation

In this thesis, simulation machines are used for running system simulations and generating results. Several link adaptation designs have been used in the simulations and each design has its own different settings of specific parameters. The description of these designs and settings of parameters are given in this chapter.

The designs are studied based on signaling reduction in random access procedure with 1) static setting, 2) dynamic setting, 3) statistic setting of parameters which are used for MCS value estimation[1] or 4) data transfer buffer size estimation.

Note that a study case with signaling reduction in releasing signaling instead of random access procedure is studied too, as a simple investigation on how much signaling reduction could contribute comparing with the LTE normal scheme.

2.1 Normal Scheme without Release Signaling

In this case[2] there is no releasing signaling in the signaling steps after the UL data transfers. A case with the complete LTE normal signaling steps is used as a reference.

The purpose is to illustrate how much potential performance this simple case could give when the UE does not require releasing signaling, comparing with LTE normal case.

[1] Note that when MCS value estimation is studied in this thesis, there is an assumption that the data transfer buffer size is assigned correctly. The purpose is to focus on the MCS values estimation performance.

[2] Actually, there may be much more signaling required due to the loss of the releasing signaling steps after UL data transfer. But as a simple comparison case in this thesis, only the potential performance is simulated.

These two schemes are evaluated in simulations. Parameters specific to this design are shown in Table 2.

TABLE 2. SIMULATIONS FOR NORMAL SCHEME WITHOUT RELEASE SIGNALING

Parameter	Value
Scheme	LTE normal scheme, LTE normal scheme without release signaling
Data transfer Packet size	{10 bytes, 50 bytes, 100 bytes, 200 bytes, 400 bytes, 600 bytes, 800 bytes, 1000 bytes}

2.2 Static MCS Design

In this design, the eNB has to estimate the MCS value assigned to the UE for UL data transfer, due to insufficient information caused by signaling reduction. Varying the fixed setting of the MCS value between simulations are used.

The purpose is to illustrate how different fixed settings of MCS value affect the performance verification such as radio resource utilization, device energy consumption, number of failure users and delay with different UL data transfers packet size.

All users in one simulation use the same fixed MCS value, and the MCS value setting is changed between simulations. Parameters specific to this design are shown in Table 3.

TABLE 3. STATIC MCS DESIGN PARAMETERS

Parameter	Value
Design name	Static MCS design
MCS value	{1, 8, 14, 28}
Data transfer Packet size	{10 bytes, 50 bytes, 100 bytes, 200 bytes, 400 bytes, 600 bytes, 800 bytes, 1000 bytes}

2.3 Dynamic MCS Design

In this design, the eNB uses a method which combines the UE transmit power with the preamble sequence number to estimate the MCS value dynamically assigned to the UE for UL data transfer. As shown in Fig. 4, when the UE generates preamble sequence which is sent to eNB in random access procedure, the preamble sequence number is chosen depending on which scale that the transmit power belongs to. At the receiving end, the eNB will figure out how large the gain-to-interference-and-noise ratio (GINR) is via calculating the path loss using the number of resource blocks, the receiving diversity, the interface noise power and some network parameters[3]. Finally, by looking up the link adaptation table with the calculated result, the eNB will assign a relevant MCS value to the UE for UL data transfer, which is explained in [4] and [5].

In the simulations, the eNB makes compensation on the estimated GINR value. If there is aggressive compensation on GINR, the assigned MCS value from the link adaptation table will be larger than that when the compensation is robust. The purpose is to illustrate how those performance verifications are affected by the different compensation settings on the estimated GINR. The table below lists the parameters specific to this design.

TABLE 4. DYNAMIC MCS DESIGN PARAMETERS

Parameter	**Value**
Design name	dynamic MCS design
Compensation	{aggressive, robust, more robust, without}
Data transfer Packet size	{10 bytes, 50 bytes, 100 bytes, 200 bytes, 400 bytes, 600 bytes, 800 bytes, 1000 bytes}

[3] When the eNB receives a preamble sequence number, it could estimate the transmit power of the UE. Then the formula $P_{\text{txpower(dB)}} - N_{\text{umber of RB}} = P_{\text{zero}} + A_{\text{lfa}} * P_{\text{athloss}} + D_{\text{eltue}}$ is used to calculate path loss, where P_{zero}, A_{lfa} and D_{eltue} are constants and the number of resource block $N_{\text{umber of RB}}$ is known by eNB.
After calculating the path loss, the formula $G_{\text{INR}} = Rx_{\text{diversity}} * P_{\text{athloss}} / (I_{\text{interface}} + N_{\text{oise}})$ is used to estimate GINR, where $\text{Rx}_{\text{diversity}}$ is the constant 2 when we use 2x2 MIMO. The cell interference and noise power per sub-band could be known at the eNB.

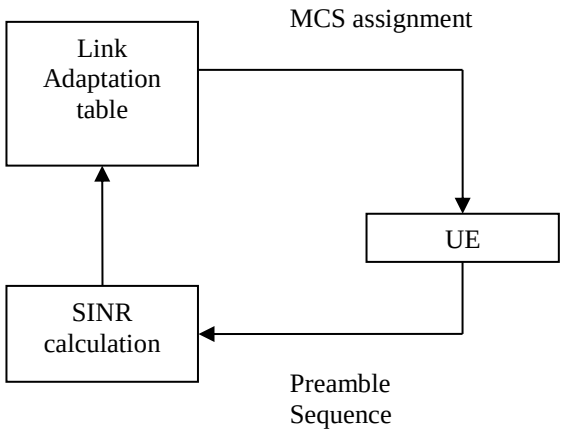

Fig. 4. Brief description of dynamic MCS design

2.4 Outer Loop MCS Design

In this design, the MCS value which is assigned to the UE is adjusted based on statistics. As shown in Fig. 5, the eNB makes use of the statistical number of MSG3 attempts per UE, which is determined through the records from all the previous UEs. If the statistical number of MSG3 attempts is larger than a target value, the eNB will decrease the MCS value assigned to the UE to guarantee that there should be less retransmission, whereas if the result is smaller than a target value, the eNB will increase the MCS value assigned to the UE to make the transmission more aggressive.

The purpose is to illustrate how different target value settings of the statistical number of MSG3 attempts per UE affect the performance verification. The target value setting is changed between simulations. Parameters specific to this design are shown in Table 5. The effect of target value setting could be seen in Appendix A.1.

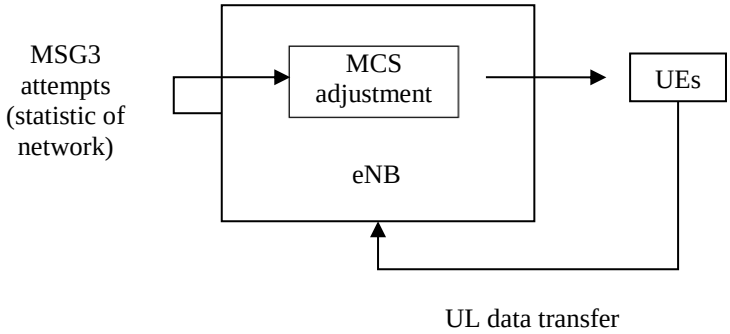

Fig. 5. Brief description of outer loop MCS design

TABLE 5. OUTER LOOP MCS DESIGN PARAMETERS

Parameter	**Value**
Design name	Outer loop MCS design
Target value	{1 MSG3 attempt , 2 MSG3 attempts}
Data transfer Packet size	{10 bytes, 50 bytes, 100 bytes, 200 bytes, 400 bytes, 600 bytes, 800 bytes, 1000 bytes}

2.5 Data Transfer Buffer Estimation Design

In this design, the eNB uses a method which combines the transfer packet size with the preamble sequence number for estimating the data transfer buffer size which is assigned to the UE for UL data transfer. As shown in Fig. 6, when the UE chooses a preamble sequence which is sent to the NB in the random access procedure, the preamble sequence number is chosen depending on which scale that the transfer packet size[4] belongs to. At the receiving end, the eNB will determine how large the transfer packet size is. Finally, the eNB could dynamically assign a data transfer packet size to the UE. Meanwhile, the MCS value is assigned by the eNB using the outer loop MCS design.

The purpose is to illustrate how the transfer buffer estimation design could affect the performance verification.

[4] In this design, the method is to combine logarithm of data transfer packet size with preamble sequence number.

Different designs are changed between simulations in order to investigate the performance of buffer size estimation. Parameters specific to this part are shown in Table 6.

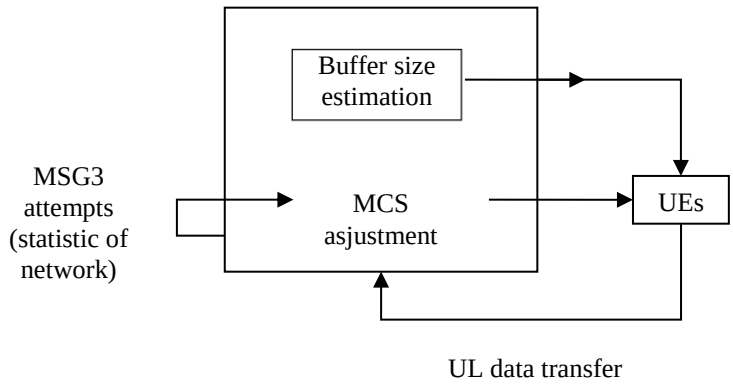

Fig. 6. Brief description of data transfer buffer estimation design

TABLE 6: SIMULATIONS FOR BUFFER ESTIMATION DESIGN

Parameter	**Value**
Design	Buffer estimation design, 6-way scheme, outer loop MCS design, LTE normal scheme
Data transfer Packet size	{10 bytes, 20 bytes, 40 bytes, 60 bytes, 80 bytes, 100 bytes, 120 byte, 140 bytes, 160 bytes, 180 bytes, 200 bytes, 220 bytes, 240 bytes, 260 bytes, 280 bytes, 300 bytes, 350 bytes, 400 bytes, 450 bytes, 500 bytes, 600 bytes, 700 bytes, 800 bytes, 900 bytes, 1000 bytes}

CHAPTER 3

3 Simulation Setup

A description of the simulation scenarios considered in this thesis is provided in this chapter.

3.1 Simulation Scenarios

In the simulations, the UEs are generated at random positions in the network. Each UE then start to move around in a random direction at a speed of 3km/h or 30km/h. Some relevant parameters are summarized in the 3GPP specification series. All simulations use a radio environment similar to 3GPP Case 1 or Case 3, with the hexagonal grid-built using 7 sites of 3 cell each.

All the simulations have the same number of UEs in the network, with heavy load background and where full buffer FTP users exist. Cell Radio-Network Temporary Identifier (C-RNTI) is assumed to be released between reports, which are periodic reporting of UL payload with a single packet.

Each simulation was run with 20 different random seeds. The results shown are from the combined statistics of all seeds.

TABLE 7. SIMULATION SCENARIOS

User distribution	Uniform
Cell layout	Hexagonal grid, 7 sites, 3 cells/site
Multi-path fading	Complex typical urban
Scheduling	Round Robin
Receiver	Maximum ratio combining
Shadow fading	Log-normal, 8dB standard deviation
Distance dependent path loss	L = 15.3+20+37.6*log(d), d = distance in meters
Acknowledgement	On application level
Traffic load	M2M UEs, heavy load background with full buffer FTP users

Transceiver antennas	2x2
System	3GPP Case 1, 3GPP Case 3
Assumption	C-RNTI released between periodic reports

3.2 Radio Resource Utilization

In the network, radio resource is limited; hence radio resource utilization is an important performance measurement, especially for those areas with many sensors but low capacity network, for example agricultural areas. In this thesis, PUSCH/PDSCH usage per UE is used to measure radio resource utilization.

A high radio resource utilization, which means a high radio interface load, leads to a small number of active UEs in the network.

The goal of this performance measurement is to illustrate how different designs based on signaling reduction could affect radio interface load.

3.3 Device Energy Consumption

It is also a challenge to prolong battery operation times of battery operated terminals especially for some sensor device types. Energy efficiency is an important factor in product competitiveness from cost and environmental perspectives.

The goal of this performance measurement is to evaluate how much of the device energy could be saved by different designs with perfect DRX or without DRX.

3.3.1 Model Structure

Figure 7 shows the components that influence device energy consumption. The purpose of each component and specific parameters are briefly described below.

Based on this model, the structure and specific model parameters of each component could be determined, as shown in Table 8 and Fig. 8, which are obtained from simulation results. This model structure was created by Ericsson Research.

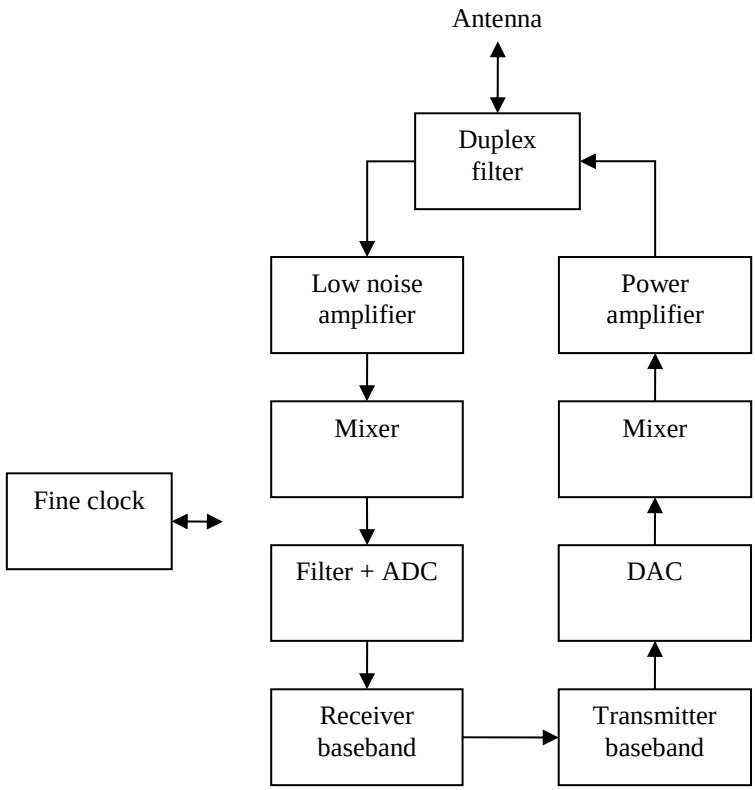

Fig. 7. Model structure of device energy consumption

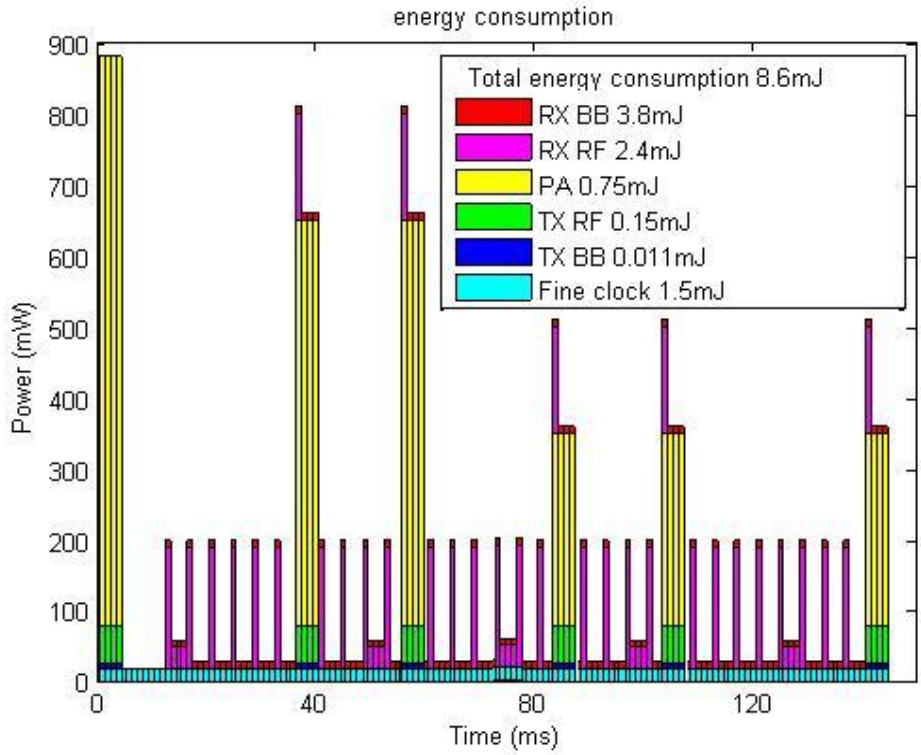

Fig. 8. Device energy consumption of each component without DRX in LTE normal scheme without releasing signaling in 3GPP Case 1

TABLE 8. DEVICE ENERGY CONSUMPTION OF EACH COMPONENT WITH PERFECT DRX AND WITHOUT DRX IN LTE NORMAL SCHEME AND WITHOUT RELEASING SIGNALING IN 3GPP CASE 1

Each component	**RX BB**	**RX RF**	**PA**	**TX RF**	**TX BB**	**Fine Clock**	**Total**	**Unit**
LTE normal scheme with perfect DRX	0.6	0.5	0.7	0.2	0.01	1.7	3.1	mJ
LTE normal scheme without DRX	4.1	2.6	0.7	0.2	0.01	1.7	9.3	mJ
No Release signaling with perfect DRX	0.3	0.2	0.8	0.2	0.01	1.5	3	mJ

No Release signaling without DRX	3.8	2.4	0.8	0.2	0.01	1.5	8.6	mJ

For the device energy consumption of each component in other study cases, please see Appendix A.2.

3.3.2 Fine Clock

Fine clock not only keeps the symbol and frame timing of the air interface but also the terminal synchronization to the air interface. It could be tuned by monitoring relevant reference signal received from the eNB, for example, the PSS and SSS in LTE.

During the receiver or transmitter operation, the fine clock must be enabled. When it is enabled, it will consume a constant power. The power consumption of the fine clock is labeled p_{fine}.

3.3.3 Receiver RF

Low noise amplifier and mixer: The low-noise amplifier (LNA) and mixer can be enabled or disabled on a symbol by symbol basis in LTE. They constitute the receiver frond end. When they are enabled, they will consume a constant power. The power consumption of the LNA and mixer at receiver is labeled $p_{\text{RX,frontend}}$

Filter and analog-to-digital converter (ADC): The filter and ADC are enabled or disabled together with the LNA and mixer, and exist in one instance per receiver branch. The power consumption of these components is assumed to be proportional to the bandwidth of the desired signal.

The power consumption of the filter and ADC is expressed as $p_{\text{RX,analog}} = B_{\text{RX}} \times k_{\text{RX,dac}}$, where B_{RX} is the signal bandwidth and $k_{\text{RX,dac}}$ is the proportionality constant. B_{RX} could be obtained from the assigned resource blocks multiplied by 180kHz ,which is the bandwidth for one RB from the simulation data.

3.3.4 Receiver Baseband

The receiver baseband performs the digital signal processing of the received signal, such as detection and synchronization, demodulation, soft buffering and combining, decoding and protocol processing.

When there is received signal, the signal processing will consume some power which includes a constant power and another part which is

proportional to bit rate. This could be expressed as $p_{RX,baseband} = p_{RX,baseband,0} + R_{RX} \times k_{RX,baseband}$, where $p_{RX,baseband,0}$ is the power of the basic parts, R_{RX} is the bit rate (Mbits/s), and $k_{RX,baseband}$ is the proportionality constant.

3.3.5 Power Amplifier (PA)

When a signal is transmitted, PA is enabled. When it is enabled, it will consume power which is nonlinear to the output power but independent of bandwidth and the PA power consumption could be expressed as $p_{TX,PA} = (L_{duplex} \times P_{TX})$ where P_{TX} is the output power and L_{duplex} is the transmit power loss for the output power in the FDD case.

3.3.6 Transmitter RF

Mixer: When a signal is transmitted, the mixer is enabled. When it is enabled, it will consume a constant power. The power consumption of the transmitter mixer is labeled $p_{TX,mixer}$.

Digital to Analog Converter (DAC): When a signal is transmitted, the DAC is enabled. When it is enabled, it will consume power which is proportional to the bandwidth of the transmitted signal. The power consumption of the DAC is expressed as $p_{TX,DAC} = B_{TX} \times k_{TX,DAC}$, where B_{TX} is the signal bandwidth and $k_{TX,DAC}$ is the proportionality constant. B_{TX} could be obtained from the assigned resource blocks multiplied by 180kHz which is the bandwidth for one RB from the simulation data.

3.3.7 Transmitter Baseband

The transmitter baseband performs the digital signal processing of the transmitted signal, such as modulation, transmit buffering coding and protocol processing.

When there is transmitted signal, the signal processing will consume some power which includes a constant power and another part which is proportional to bit rate. This could be expressed as $p_{TX,baseband} = p_{TX,baseband,0} + R_{TX} \times k_{TX,baseband}$, where $p_{TX,baseband,0}$ is the power of the basic parts, R_{TX} is the bit rate (Mbits/s), and $k_{TX,\ baseband}$ is the proportionality constant.

3.3.8 Model Parameters

The following parameters are based on estimated power consumption of the state of the art mobile platforms. Although the different kinds of sensors have different model parameters, to simplify the problem, in this thesis, the following specific model parameters are used to analyze the sensor energy consumption.

TABLE 9. MODEL PARAMETERS

Parameter	Unit	Value
$p_{application}$	mW	3.2
p_{coarse}	mW	0.36
p_{fine}	mW	10
$p_{RX,frontend}$	mW	72
$k_{RX,analog}$	mW/MHz	14
$p_{RX,baseband,0}$	mW	25
$k_{RX,baseband}$	mW/Mbps	7
$p_{TX,PA}$	mW	$72 + 17.5 P_{TX}^{0.784}$
$p_{TX,mixer}$	mW	80
$k_{TX,DAC}$	mW/MHz	16
$p_{TX,baseband,0}$	mW	11
$k_{TX,baseband}$	mW/Mbps	1
L_{duplex}	dB	2

3.4 Failure Users

It is necessary to measure the number of failure users, for whom retransmission attempts failed in the network. A high number of failure users leads to a poor QoS whereas there could be a good Qos if no failure users exist in the network.

The goal of this performance measurement is to illustrate how many failure users could be caused by different designs based on signaling reduction in the simulations.

3.5 Delay

The delay could be defined as $D_t = T_e - T_a$. The delay of the UE is denoted as D_t, T_a is the start time when the UE begins sending preamble sequence to start the random access and T_e is the end time when the UE completes the transmission and reception tasks.

Delay is an important measurement to verify whether the RRM is efficient or not. If without a proper link adaptation, the delay will be longer so that it could waste the device's energy and do not release the radio resource in time.

The goal of this performance measurement is to study how different designs based on signaling reduction affect delay.

CHAPTER 4

4 Simulation Results

4.1 Radio Resource Utilization

In this section, the radio resource utilization is shown together with the average and 95th percentile usage per UE. It can be seen from the figures (e.g., Fig. 27, Fig. 28 and Fig. 29) that when there is signaling reduction in the random access procedure with proper settings of specific parameters, the radio resource usage will be a lot more efficient than that in the LTE normal scheme. When even the release signaling reduction is used in the LTE normal scheme, there could be more efficient performance on the PDSCH usage. There is much more efficient radio resource usage when the simulations run in the 3GPP Case 1 radio environment than that in 3GPP Case 3, because the cell size in Case 1 is much smaller than that in Case 3.

Note that the y axes differ between different designs because the plots are zoomed in on the relevant parts for each design case.

4.1.1 Normal scheme without release signaling Case 1

The average PUSCH usage, 95th percentile PUSCH usage and average PDSCH usage per UE are shown in Figs. 9, 10 and 11, respectively.

From Figs. 9-11, it could be seen that there is almost no difference on the performance of PUSCH usage but obvious difference on the performance of PDSCH usage between the two schemes. This could be explained by that in this simple signaling reduction scheme there is no reduction on the uplink signaling but only reduction on the downlink release signaling.

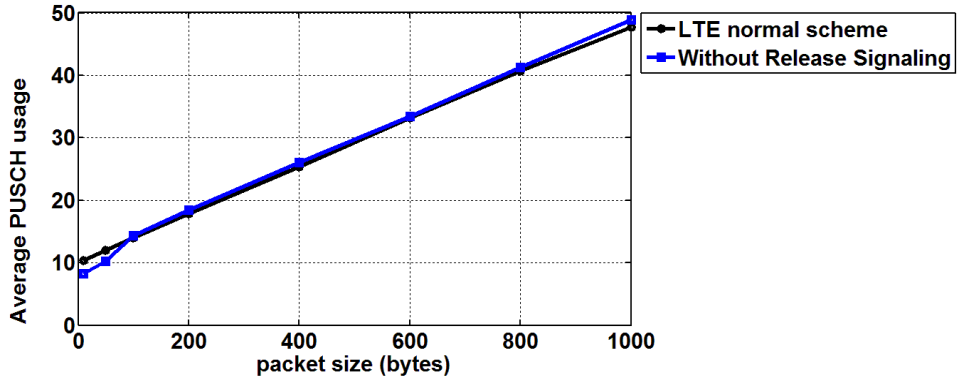

Fig. 9. Average PUSCH usage

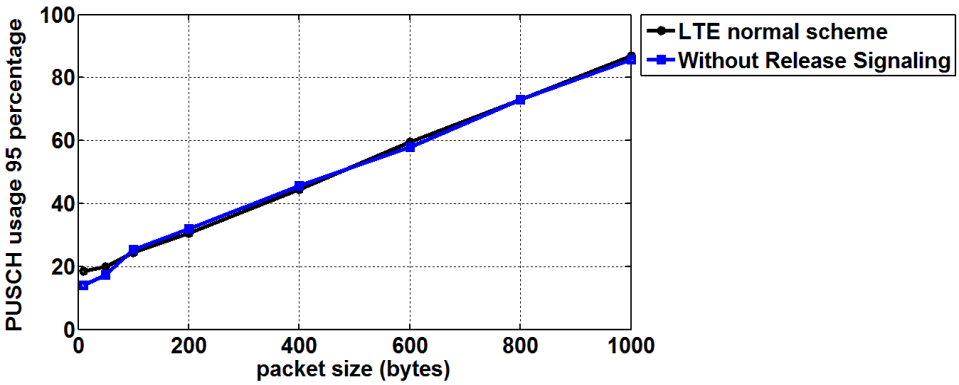

Fig. 10. 95^{th} percentile PUSCH usage

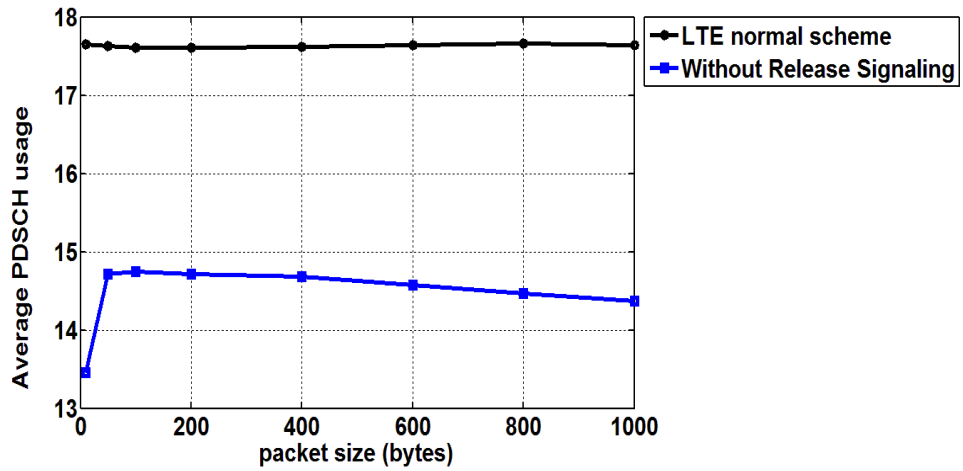

Fig. 11. Average PDSCH usage

4.1.2 Normal scheme without release signaling Case 3

The average PUSCH usage, 95th percentile PUSCH usage and average PDSCH usage per UE are shown in Fig. 12, 13 and 14, respectively.

From Figs. 12-14, we see there is almost no difference on the performance of PUSCH usage but obvious difference on the performance of PDSCH usage between the two schemes. This could be also explained by that there is no reduction on the uplink signaling in the simple signaling reduction scheme but only reduction on the downlink release signaling.

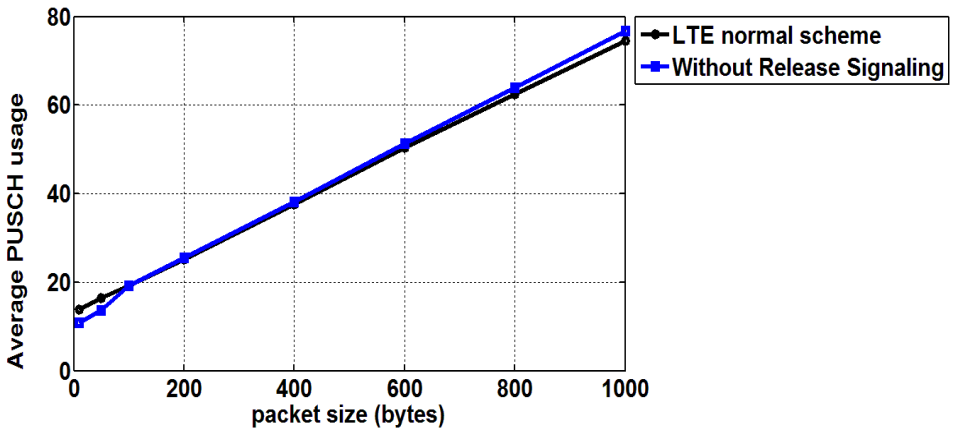

Fig. 12. Average PUSCH usage

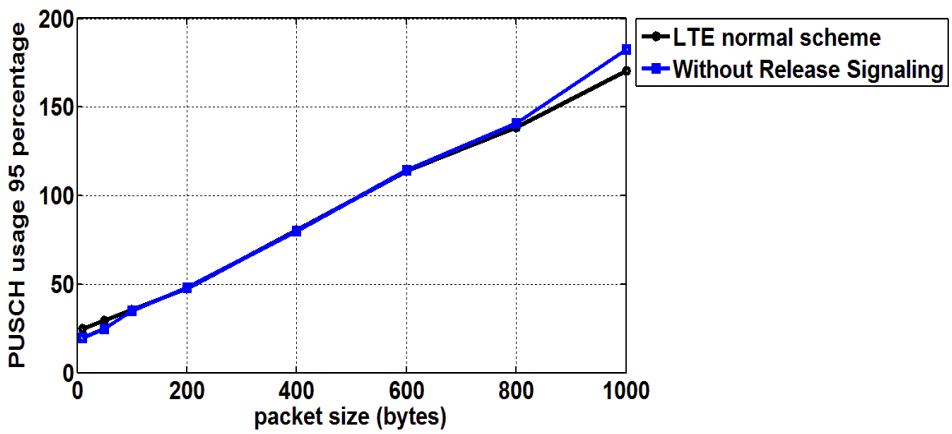

Fig. 13. 95th percentile PUSCH usage

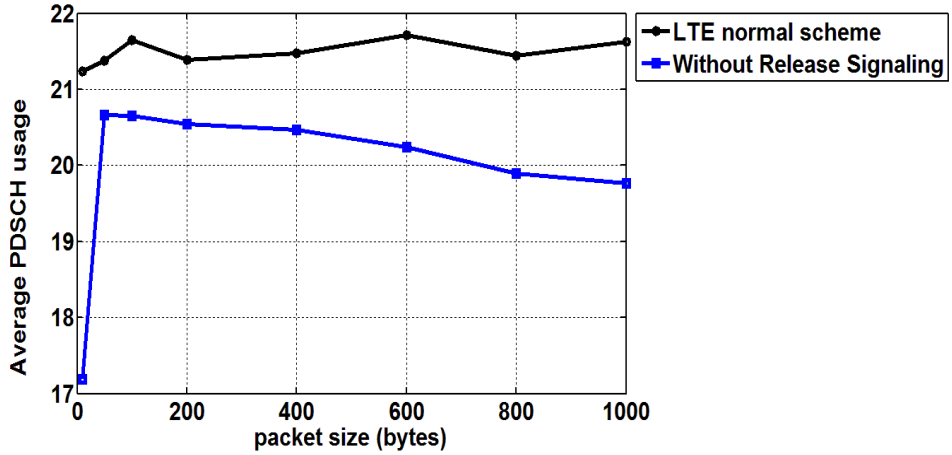

Fig. 14. Average PDSCH usage

4.1.3 Static MCS design Case 1

The average PUSCH usage and 95th percentile PUSCH usage per UE are shown in Fig. 15 and 16, respectively.

From Figs. 15 and 16, we see that the design with more aggressive MCS value setting (i.e., higher values) has better performance on the PUSCH usage. But taking into account the performance on failure users, in Fig. 75, it could be seen that there will be much more failure rate in the network when the most aggressive MCS value setting is used. Hence, the MCS value of 14 gives a good tradeoff between these two performance criteria.

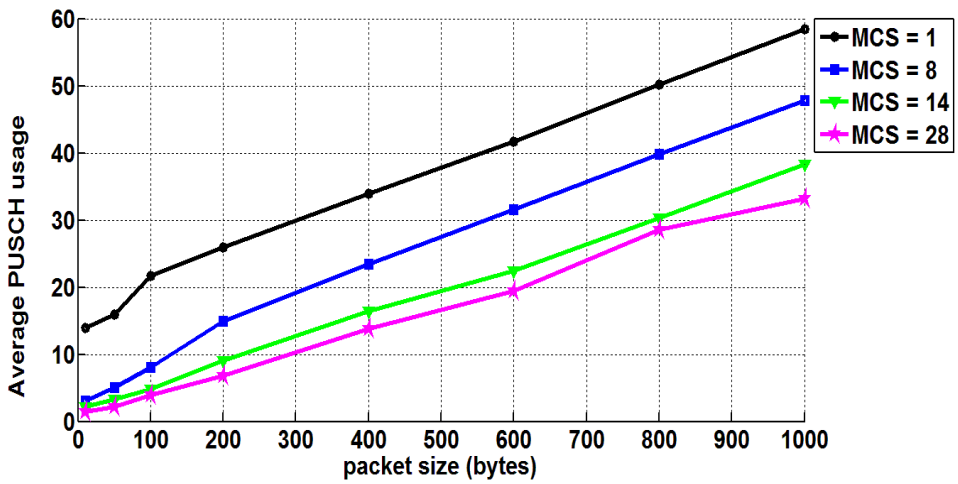

Fig. 15. Average PUSCH usage

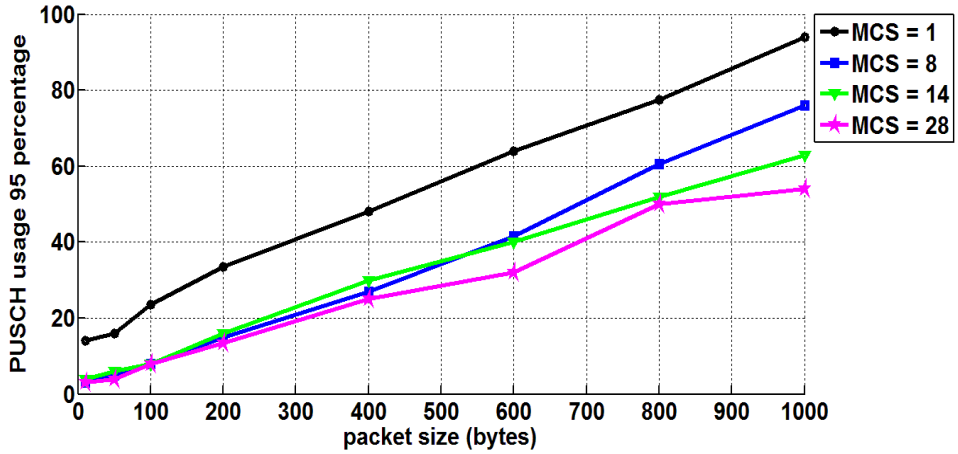

Fig. 16. 95th percentile PUSCH usage

4.1.4 Static MCS design Case 3

The average PUSCH usage and 95th percentile PUSCH usage per UE are shown in Figs 17 and 18, respectively. Similar trends as in static MCS design Case 1 is observed in Case 3.

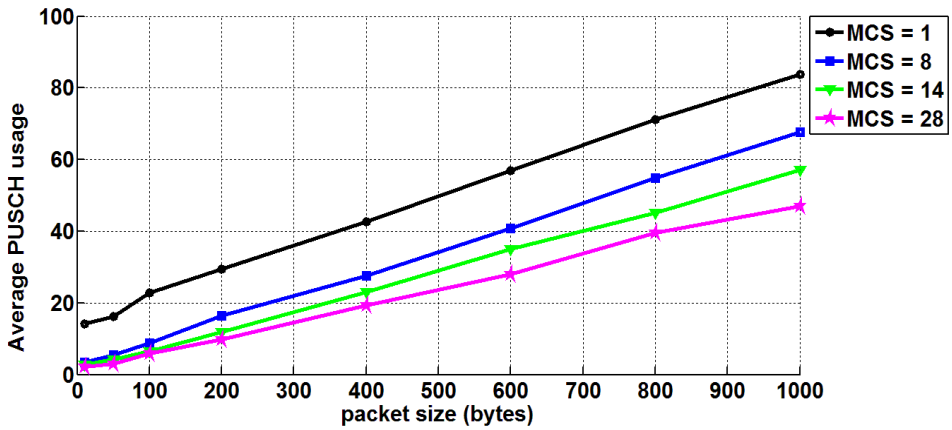

Fig. 17. Average PUSCH usage

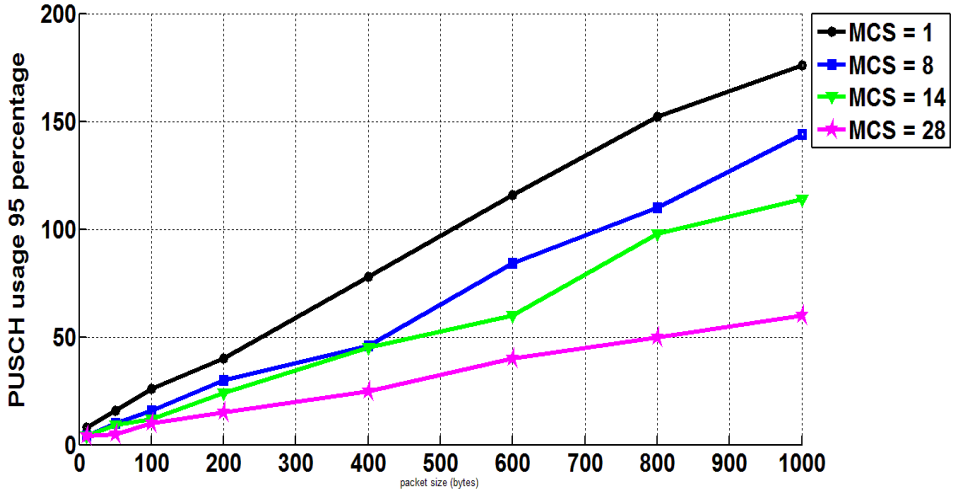

Fig. 18. 95th percentile PUSCH usage

4.1.5 Dynamic MCS design Case 1

The average PUSCH usage and 95th percentile PUSCH usage per UE are shown in Figs. 19 and 20, respectively.

From Figs. 19 and 20, we see that the design with aggressive compensation setting has better performance on the PUSCH usage. The reason is that with aggressive compensation setting, a higher MCS value could be assigned to the UE, so that the design could have more efficiency on the resource usage. But taking into account the performance on energy consumption seen in Fig. 49 and failure users seen in Fig. 77, it could be seen that there will be much more energy consumption and failure rate in the network when the aggressive compensation setting is used.

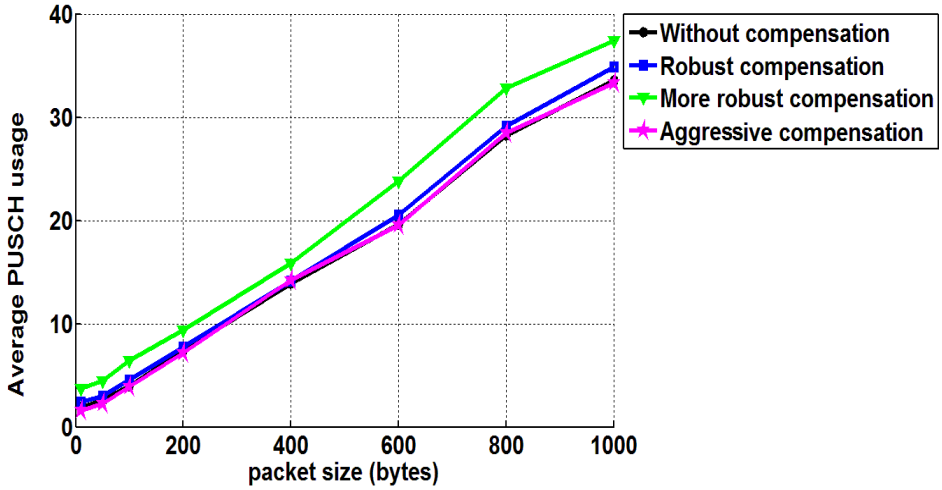

Fig. 19. Average PUSCH usage

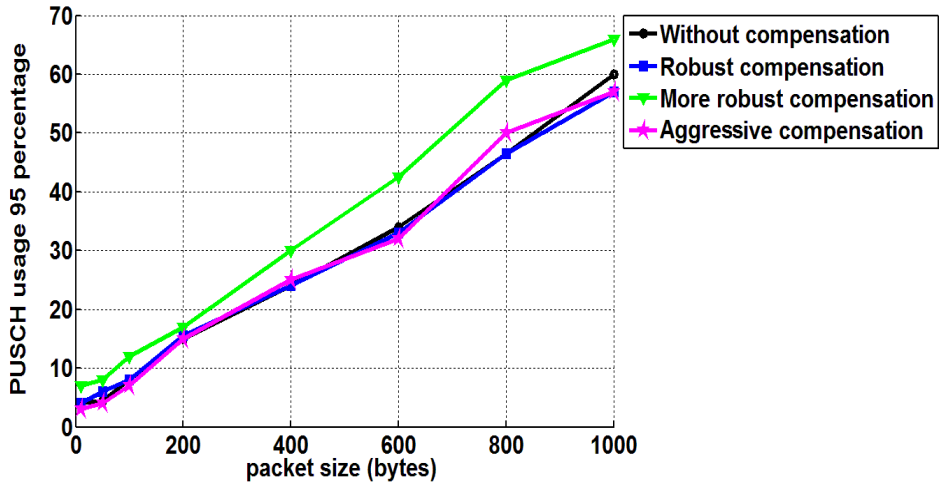

Fig. 20. 95th percentile PUSCH usage

4.1.6 Dynamic MCS design Case 3

The average PUSCH usage and 95th percentile PUSCH usage per UE are shown in Figs. 21 and 22, respectively. Similar trends as in dynamic MCS design Case 1 is observed in Case 3, except that the relative performance of the design with robust compensation is poorer than in that in Case 1.

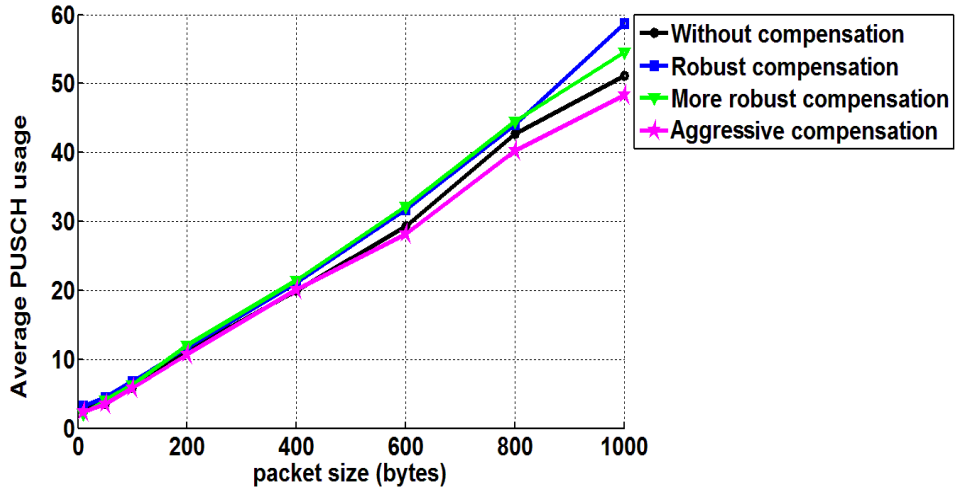

Fig. 21. Average PUSCH usage

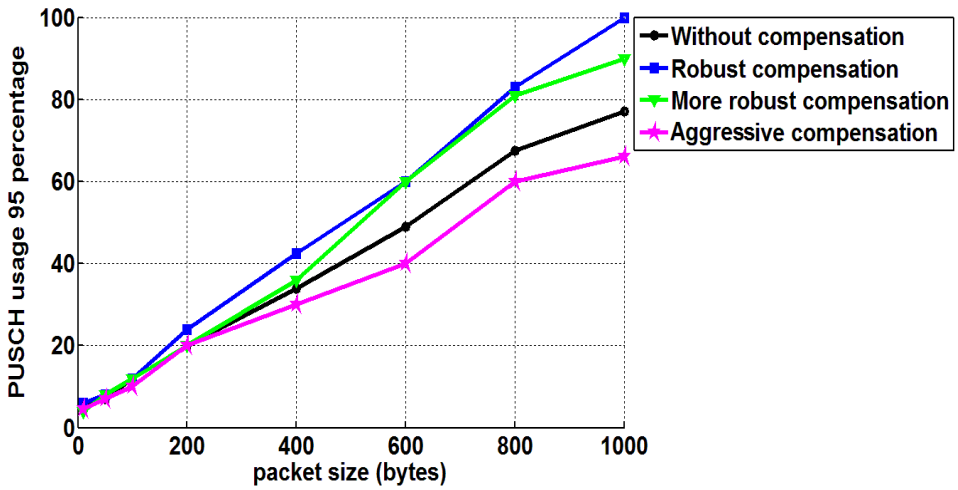

Fig. 22. 95th percentile PUSCH usage

4.1.7 Outer loop MCS design Case 1

The average PUSCH usage and 95th percentile PUSCH usage per UE are shown in Figs. 23 and 24, respectively. The setting with 2 MSG3 attempts target gives better PUSCH usage performance in general, especially at larger packet sizes.

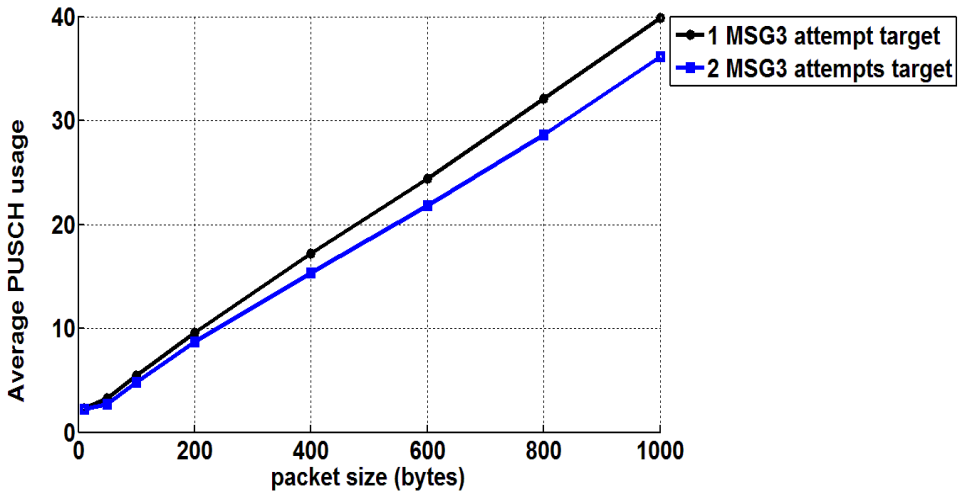

Fig. 23. Average PUSCH usage

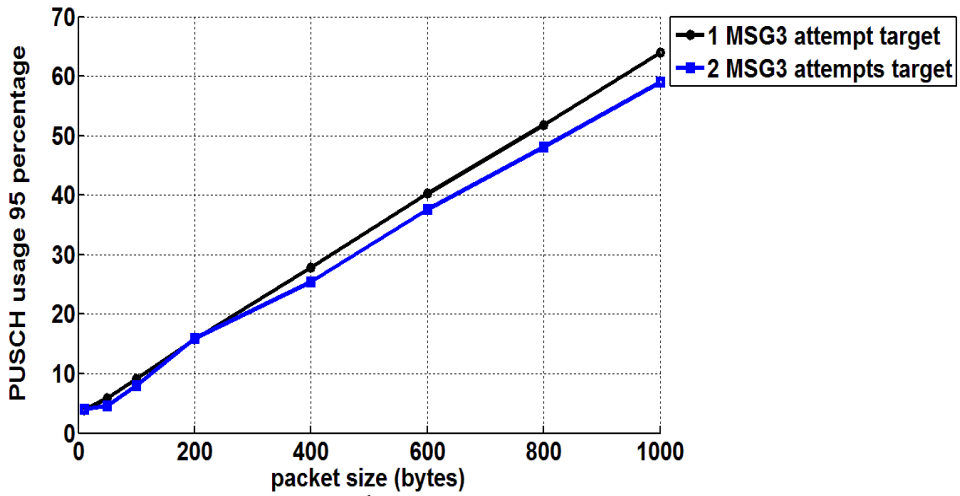

Fig. 24. 95th percentile PUSCH usage

4.1.8 Outer loop MCS design Case 3

The average PUSCH usage and 95th percentile PUSCH usage per UE are shown in Figs. 25 and 26, respectively. Similar trends as in outer loop MCS design Case 1 can be observed in these figures.

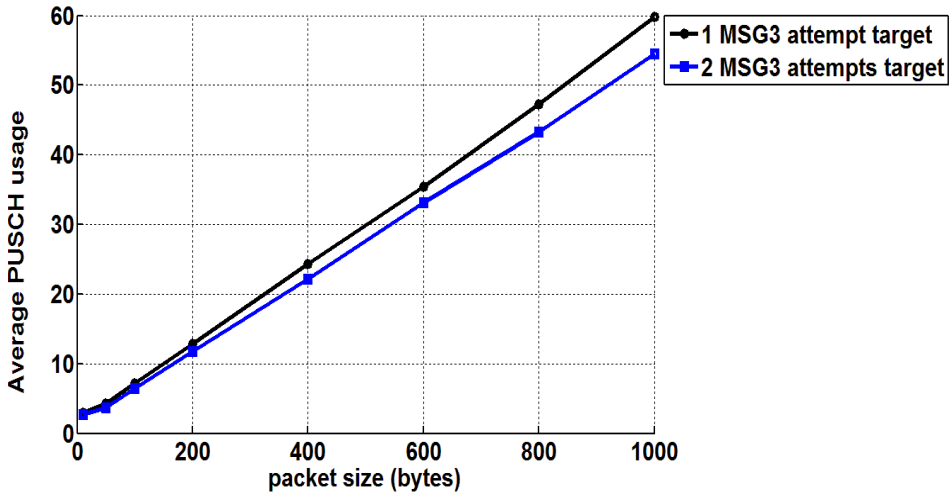

Fig. 25. Average PUSCH usage

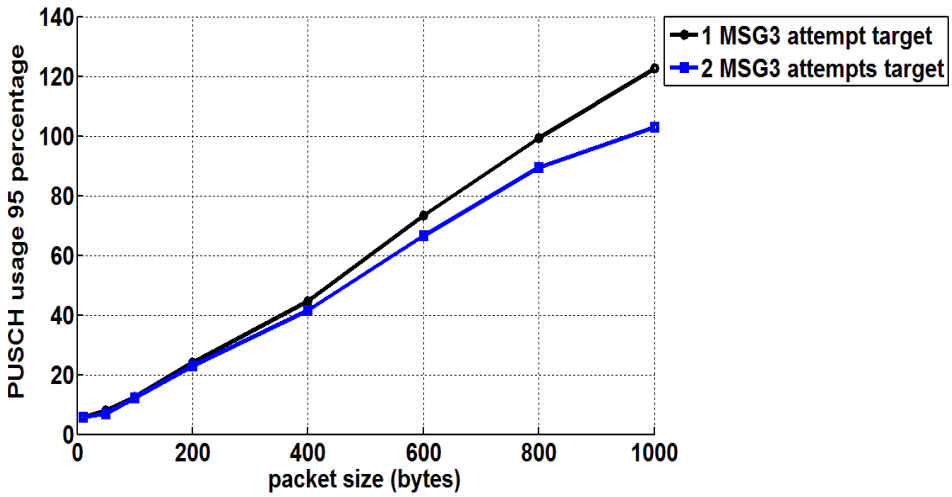

Fig. 26. 95th percentile PUSCH usage

4.1.9 Data transfer buffer estimation design Case 1

The average PUSCH usage, 95th percentile PUSCH usage and average PDSCH usage per UE are shown in Figs. 27, 28 and 29, respectively. The 2-MSG3 attempts target setting is chosen as the parameter for the outer loop MCS design.

From Figs. 27-29, it can be seen that when there is signaling reduction in the random access procedure with proper settings of specific parameters, the radio resource usage will be much more efficient than that in the LTE normal scheme.

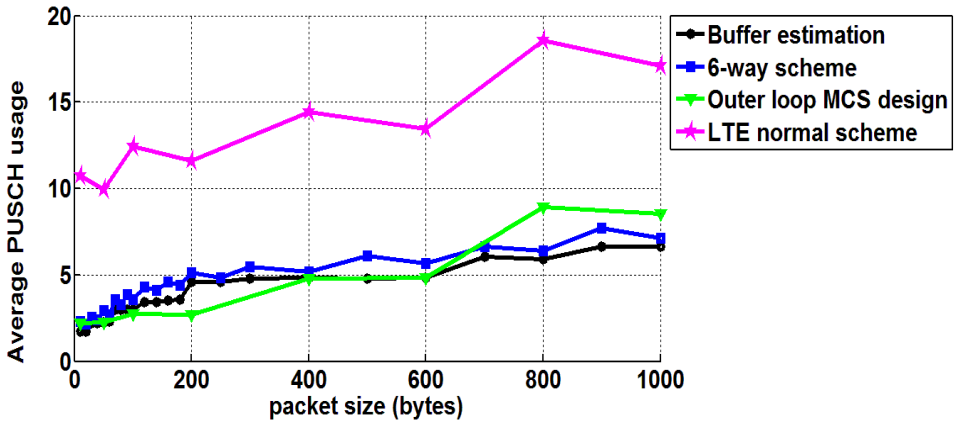

Fig. 27. Average PUSCH usage

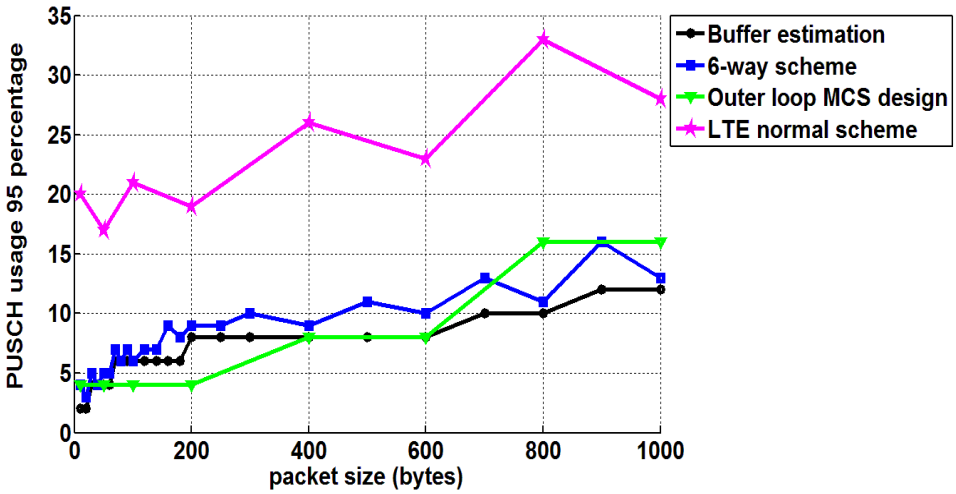

Fig. 28. 95th percentile PUSCH usage

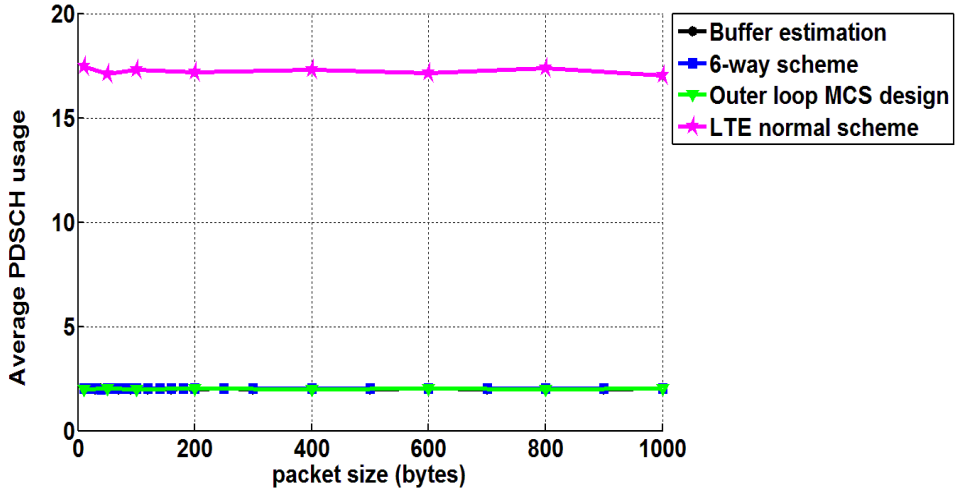

Fig. 29. Average PDSCH usage

4.1.10 Data transfer buffer estimation design Case 3

The average PUSCH usage, 95th percentile PUSCH usage and average PDSCH usage per UE are shown in Figs. 30, 31, and 32, respectively. Although in general the absolute PDSCH usage is higher in Case 3 as compared to Case 1, due to more efficient radio resource usage for the smaller cell size of Case 1, the relative trends between the curves in these two cases are similar.

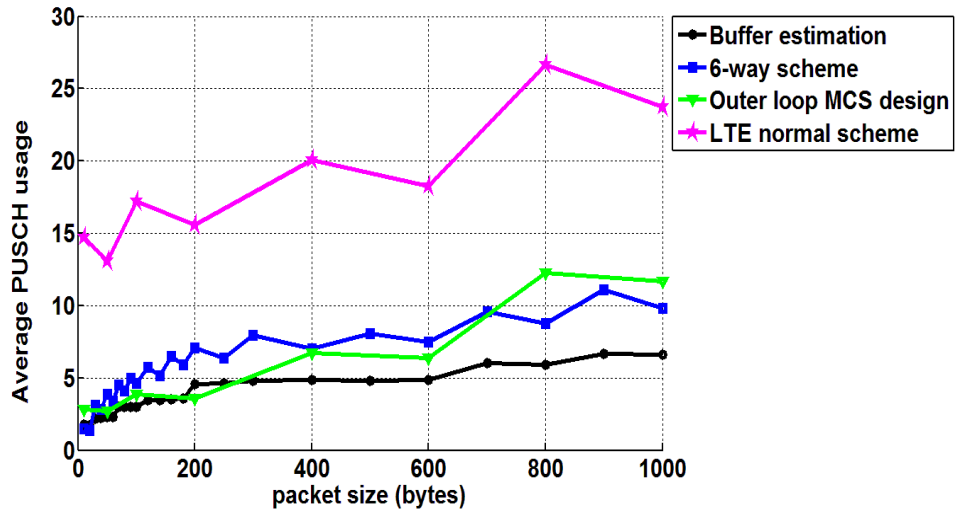

Fig. 30. Average PUSCH usage

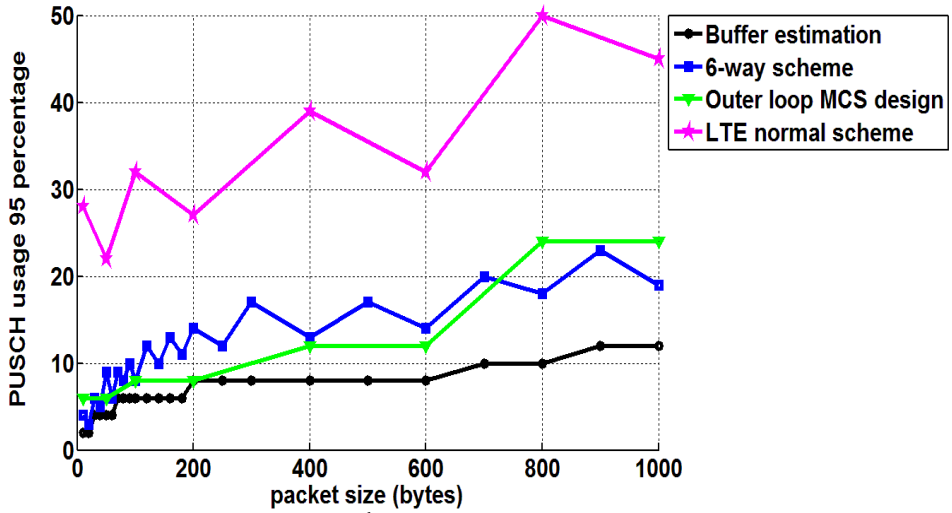

Fig. 31. 95th percentile PUSCH usage

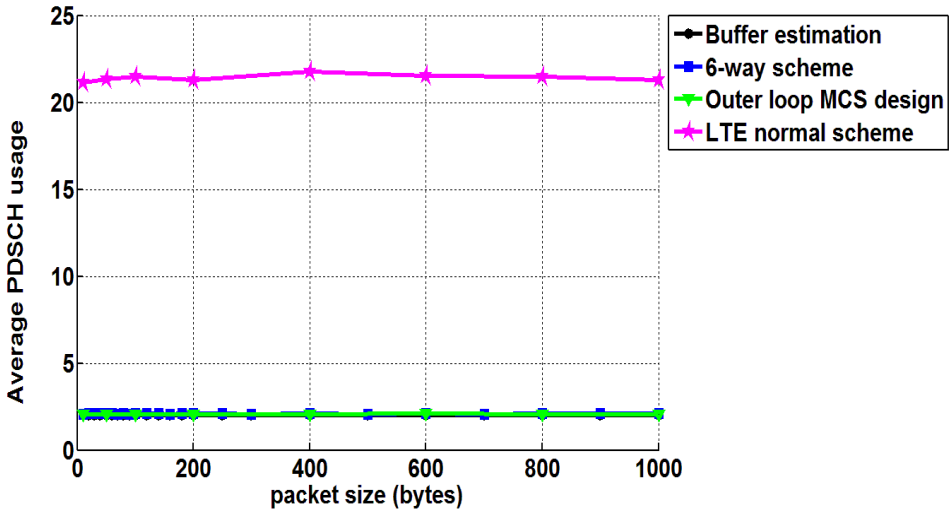

Fig. 32. Average PDSCH usage

4.2 Device Energy Consumption

The device energy consumption is shown together with the average and 95th percentile device energy consumption per UE during its delay. There is much more efficient device energy consumption resource usage when the simulations run in the 3GPP Case 1 radio environment than that in 3GPP Case 3 because the cell size in Case 1 is much smaller than that in Case 3.

Note that the y axes differ between the different designs because the plots are zoomed in on the relevant parts for each design case.

4.2.1 Normal scheme without release signaling Case 1

The average device energy consumption per UE without DRX, 95th percentile device energy consumption without DRX, average device energy consumption with perfect DRX and 95th percentile device energy consumption with perfect DRX are shown in Figs. 33, 34, 35 and 36, respectively.

The results show that there is potentially better performance under the normal scheme without release signaling than the normal scheme due to the reduction on the signaling.

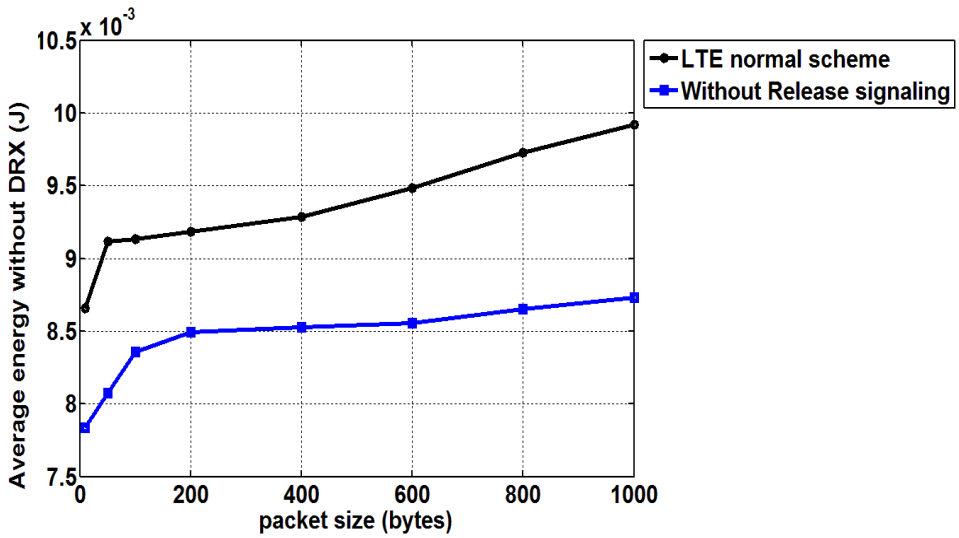

Fig. 33. Average device energy consumption without DRX

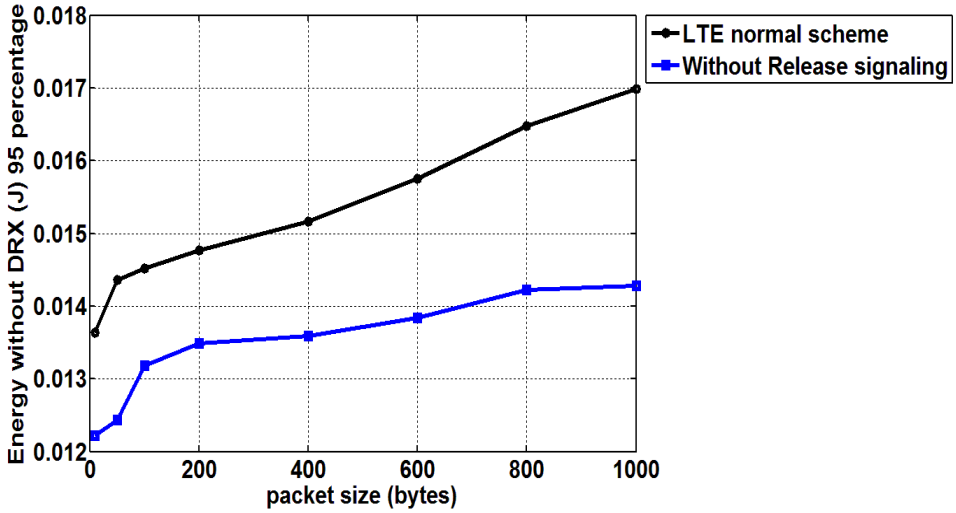

Fig. 34. 95th percentile device energy consumption without DRX

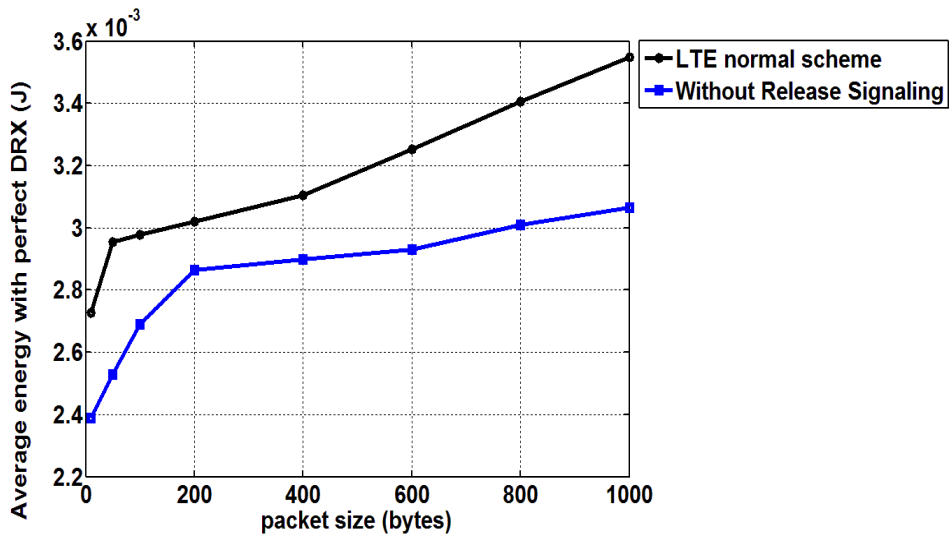

Fig. 35. Average percentile device energy consumption with perfect DRX

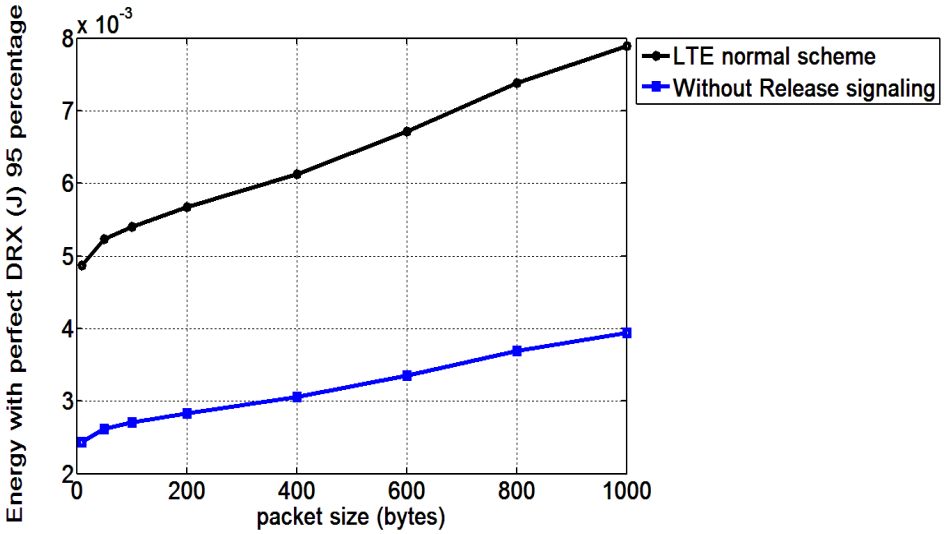

Fig. 36. 95th percentile device energy consumption with perfect DRX

4.2.2 Normal scheme without release signaling Case 3

The average device energy consumption per UE without DRX, 95th percentile device energy consumption without DRX, average device energy consumption with perfect DRX and 95th percentile device energy consumption with perfect DRX are shown in Figs 37, 38, 39 and 40, respectively. Similar trends as in Case 1 are seen here, except that the performance advantage in percentage is notably smaller in Figs 38 and 39.

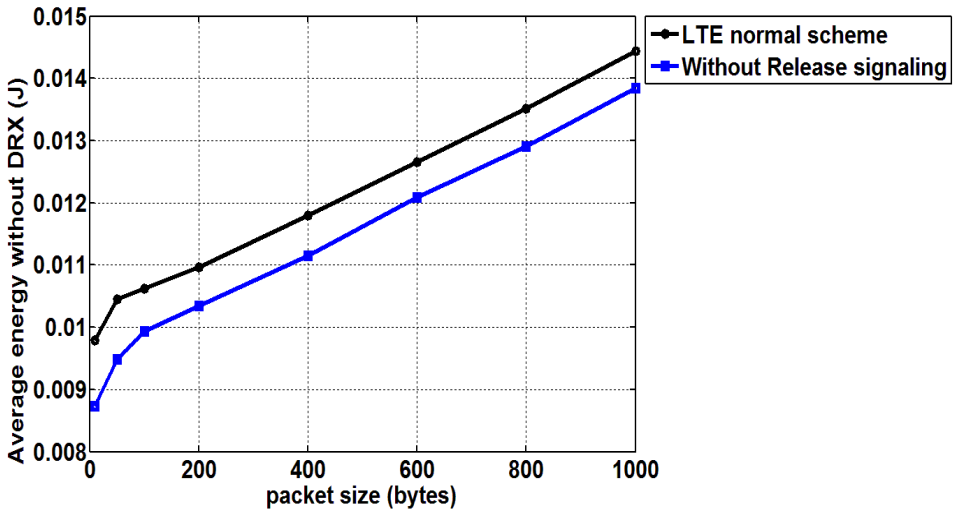

Fig. 37. Average device energy consumption without DRX

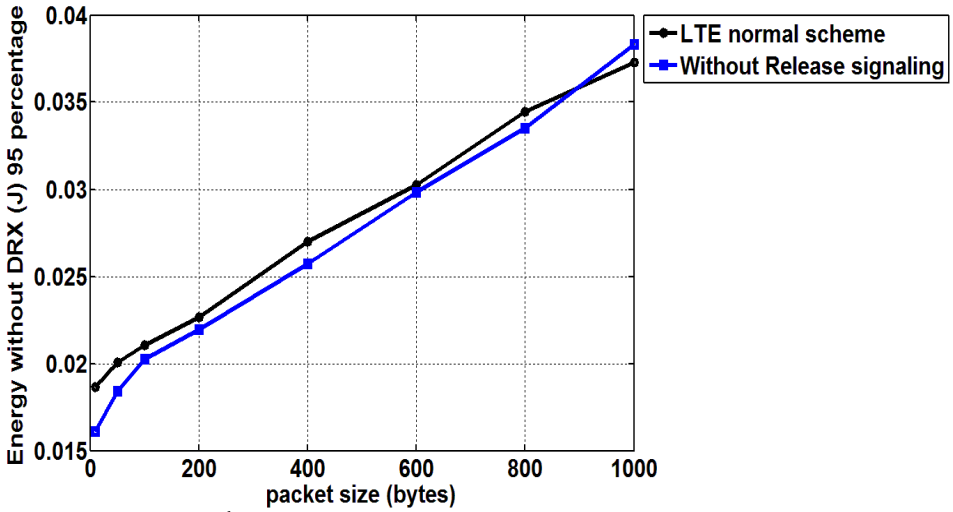

Fig. 38. 95th percentile device energy consumption without DRX

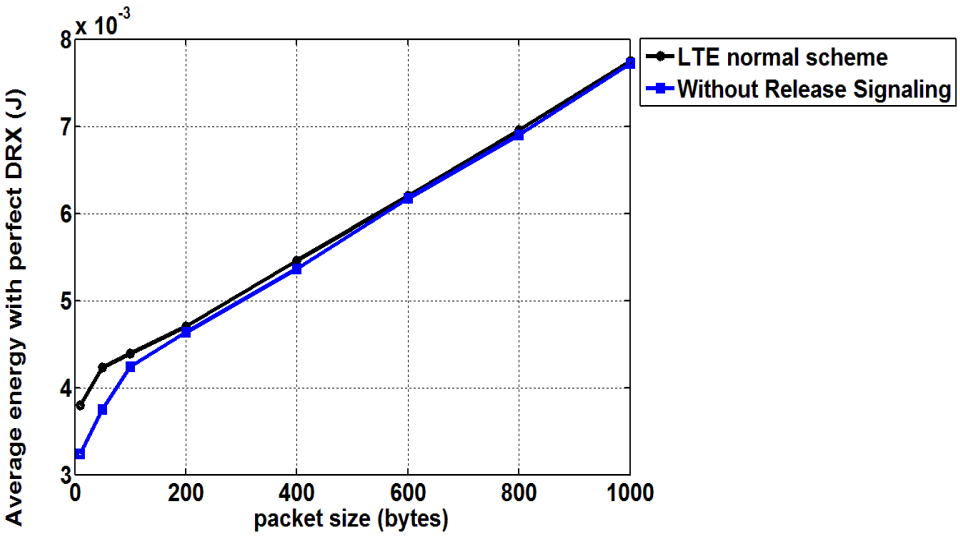

Fig. 39. Average percentile device energy consumption with perfect DRX

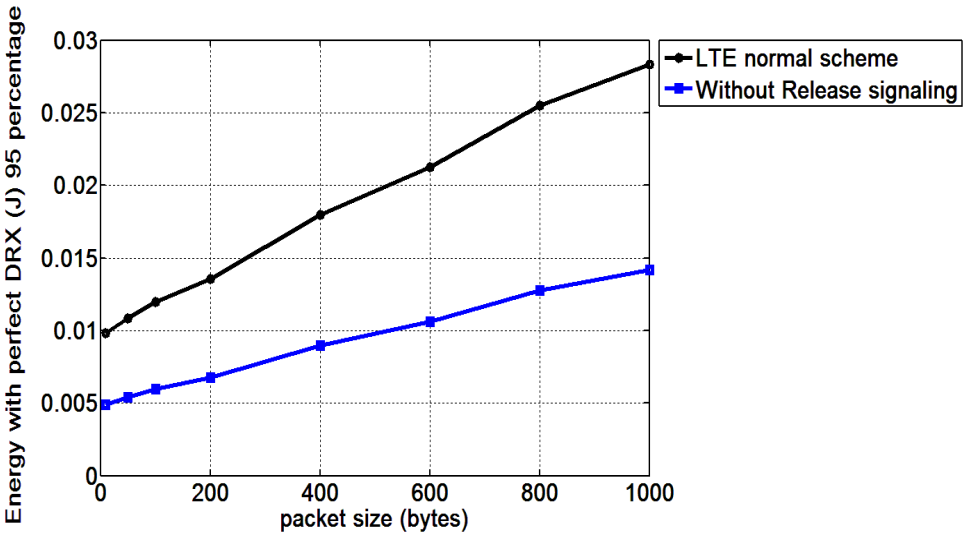

Fig. 40. 95th percentile device energy consumption with perfect DRX

4.2.3 Static MCS design Case 1

The average device energy consumption per UE without DRX, 95th percentile device energy consumption without DRX, average device energy consumption with perfect DRX and 95th percentile device energy consumption with perfect DRX are shown in Figs. 41, 42, 43 and 44, respectively.

The results show that there is potentially better performance under the design with the setting of MCS = 14. The reason is that with this proper MCS value setting, the design has better performance on the number of data transfer attempts and delay (see Fig. 85), so that it offers more efficient energy consumption.

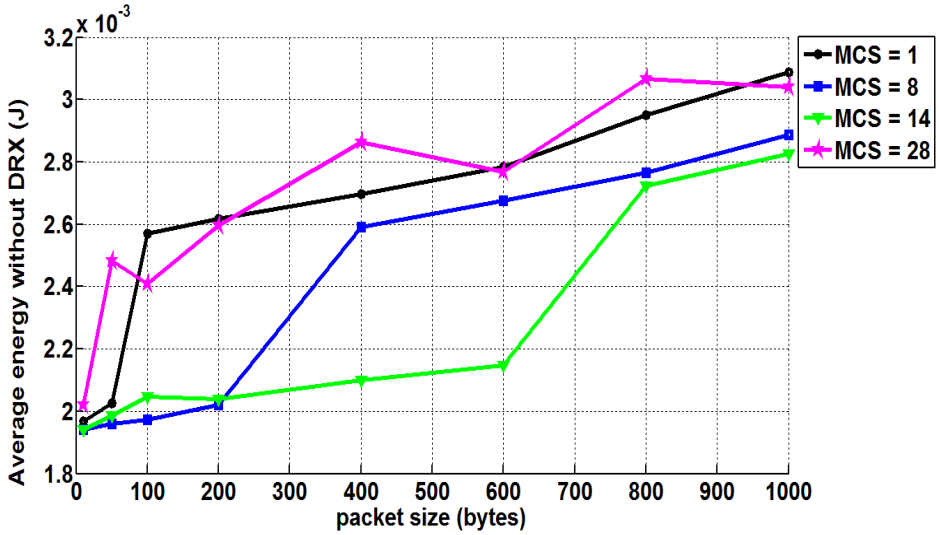

Fig. 41. Average device energy consumption without DRX

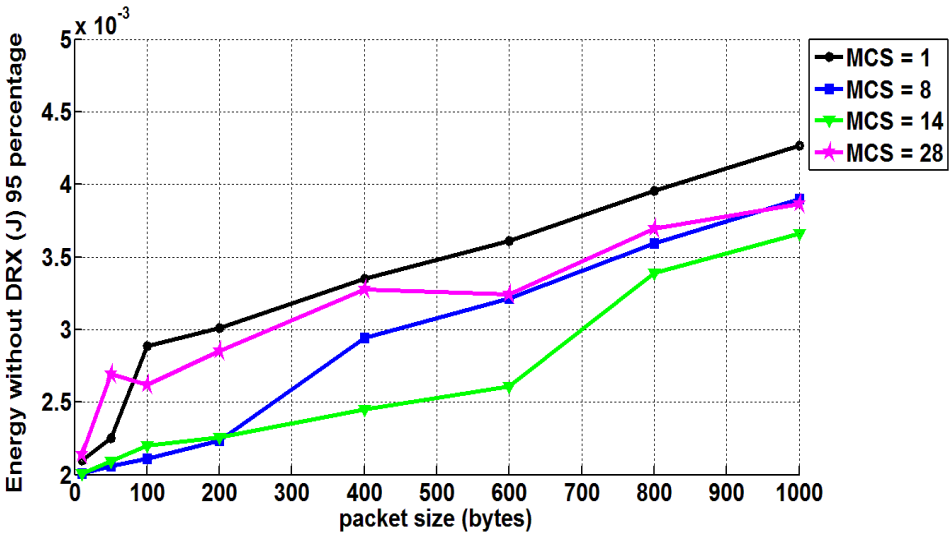

Fig. 42. 95th percentile device energy consumption without DRX

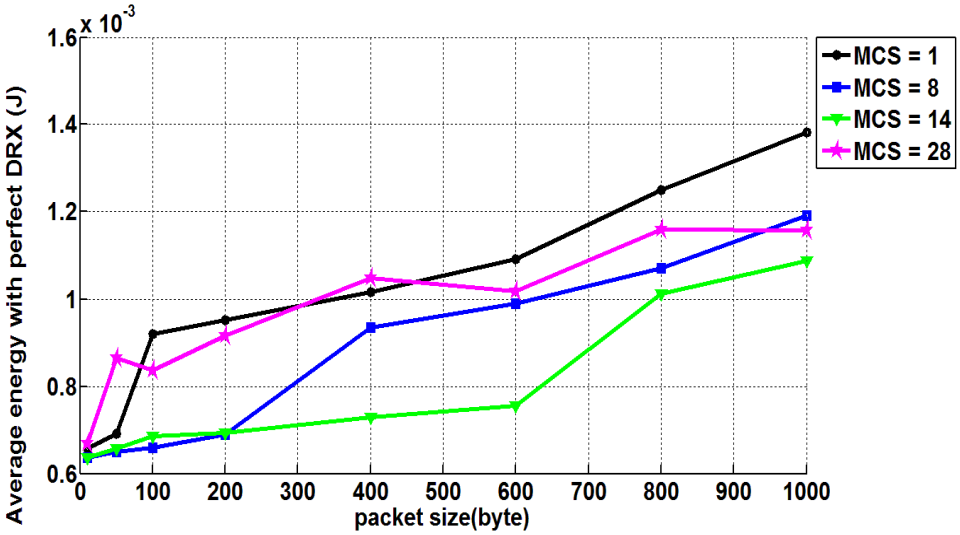

Fig. 43. Average percentile device energy consumption with perfect DRX

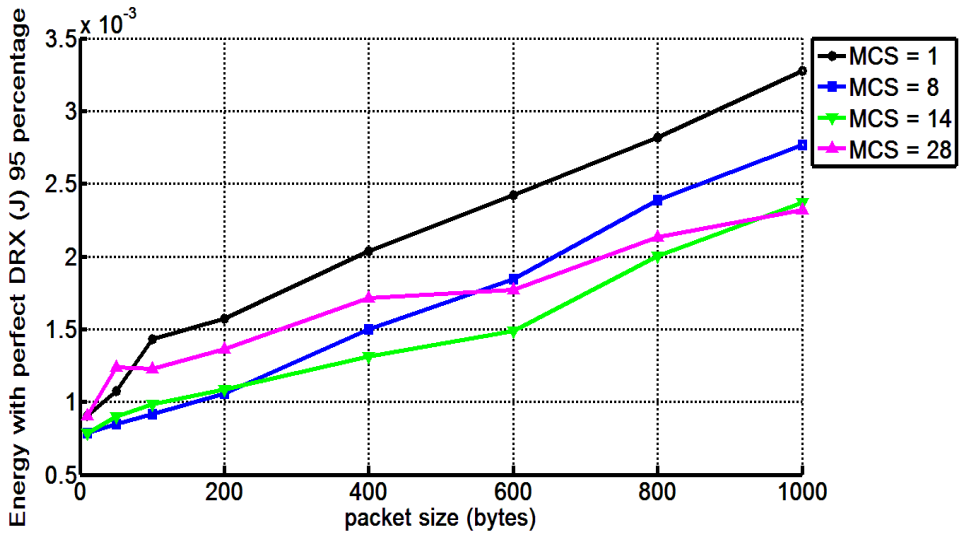

Fig. 44. 95th percentile device energy consumption with perfect DRX

4.2.4 Static MCS design Case 3

The average device energy consumption per UE without DRX, 95th percentile device energy consumption without DRX, average device energy consumption with perfect DRX and 95th percentile device energy consumption with perfect DRX are shown in Figs. 45, 46, 47 and 48, respectively. As for Case 1, the setting with MCS = 14 provides the best overall performance.

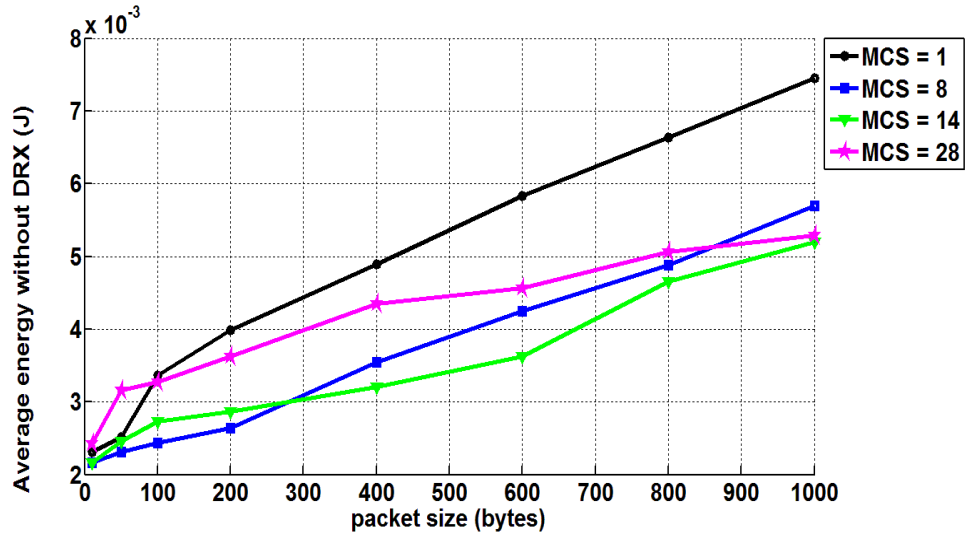

Fig. 45. Average device energy consumption without DRX

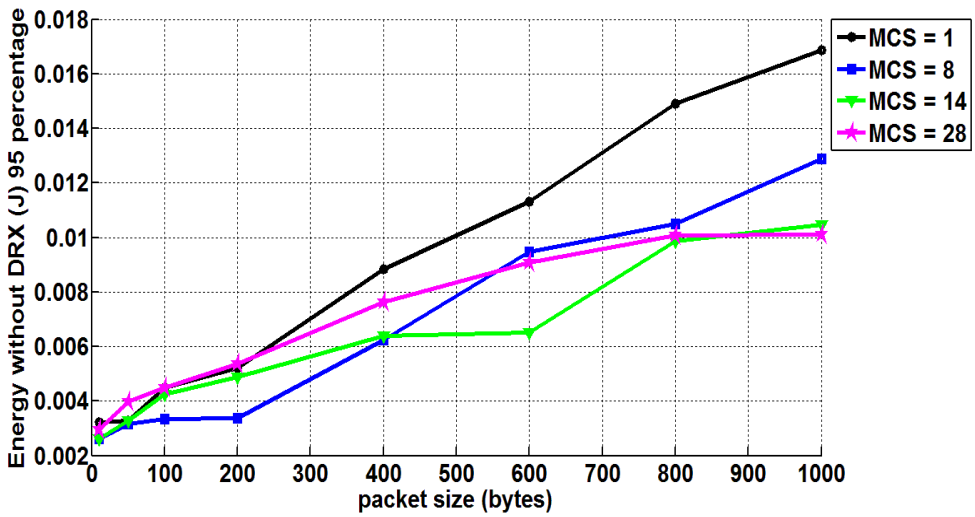

Fig. 46. 95th percentile device energy consumption without DRX

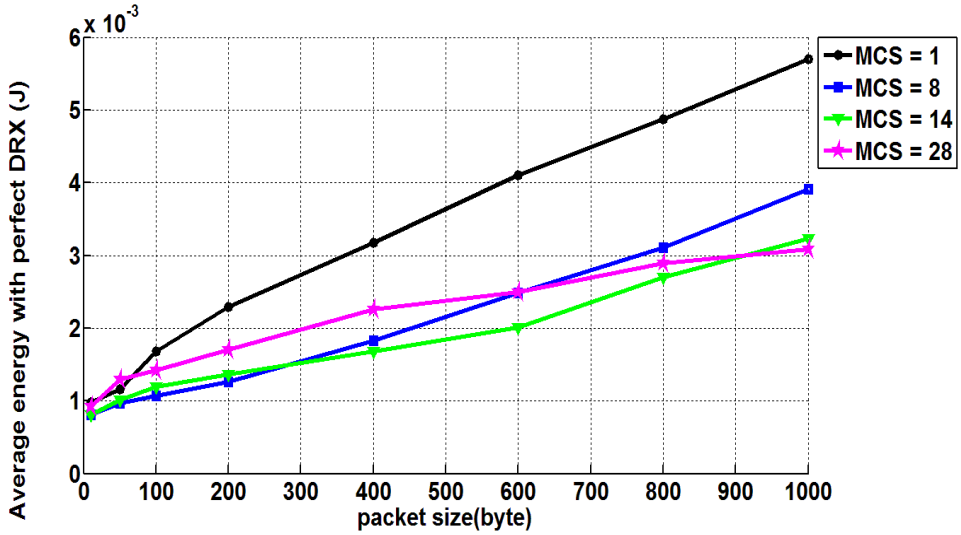

Fig. 47. Average percentile device energy consumption with perfect DRX

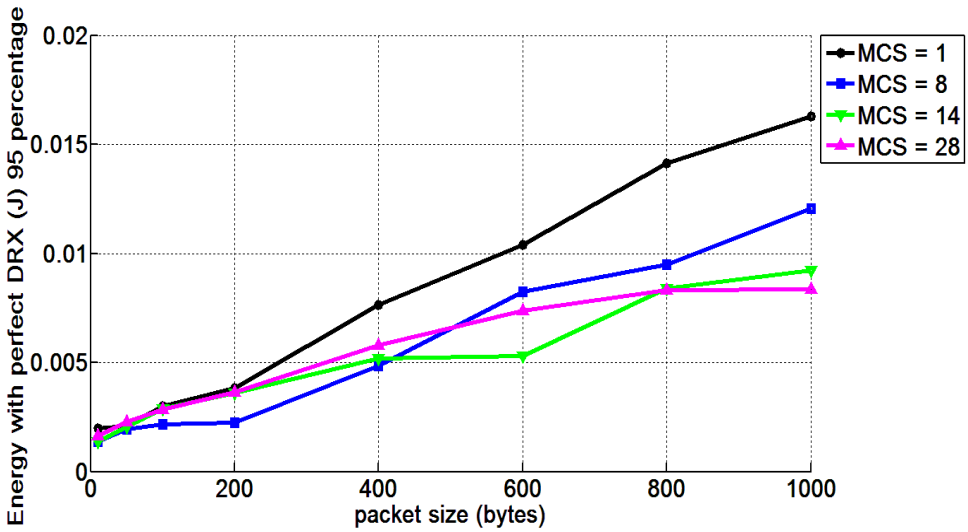

Fig. 48. 95th percentile device energy consumption with perfect DRX

4.2.5 Dynamic MCS design Case 1

The average device energy consumption per UE without DRX, 95th percentile device energy consumption without DRX, average device energy consumption with perfect DRX and 95th percentile device energy consumption with perfect DRX are shown in Figs. 49, 50, 51 and 52, respectively. The results show that there is potentially better performance on energy consumption under the design with robust (or more robust) compensation setting than that with aggressive compensation setting.

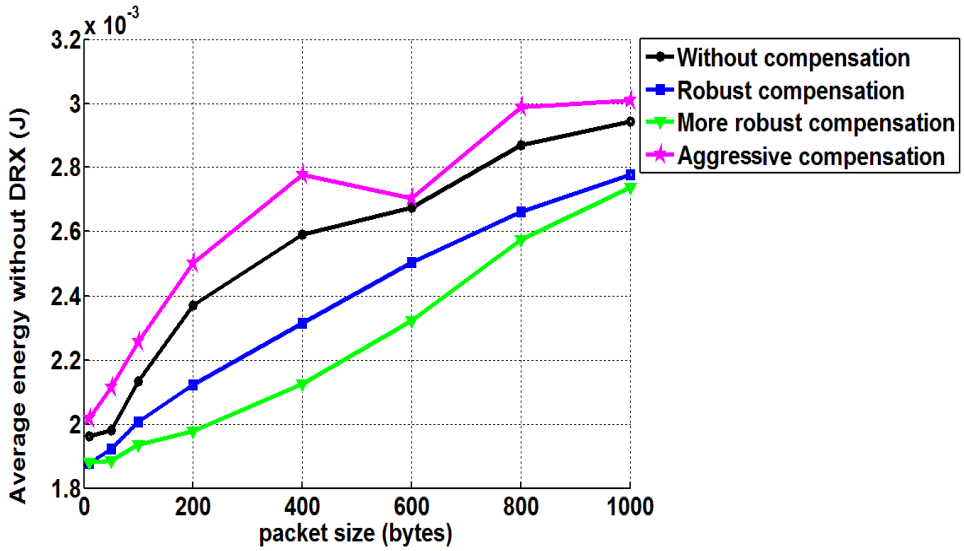

Fig. 49. Average device energy consumption without DRX

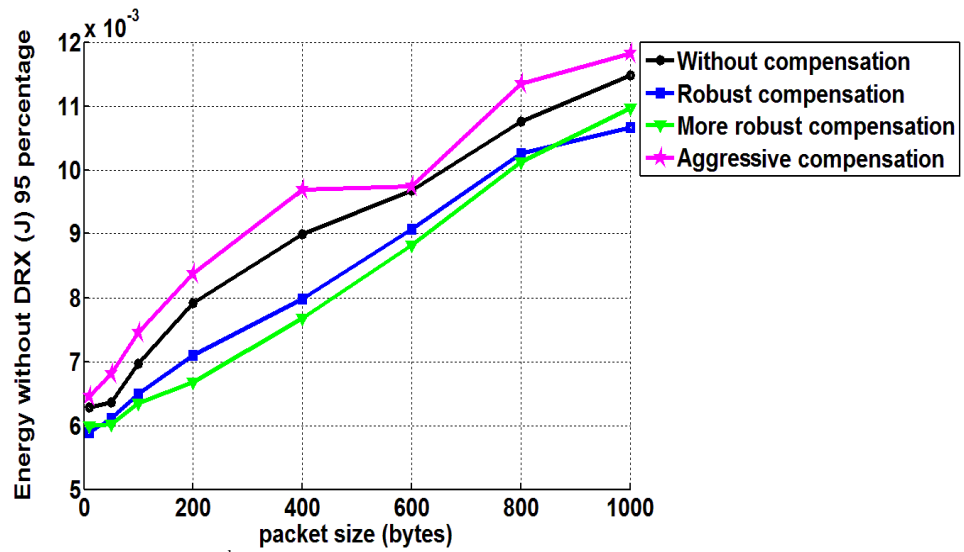

Fig. 50. 95th percentile device energy consumption without DRX

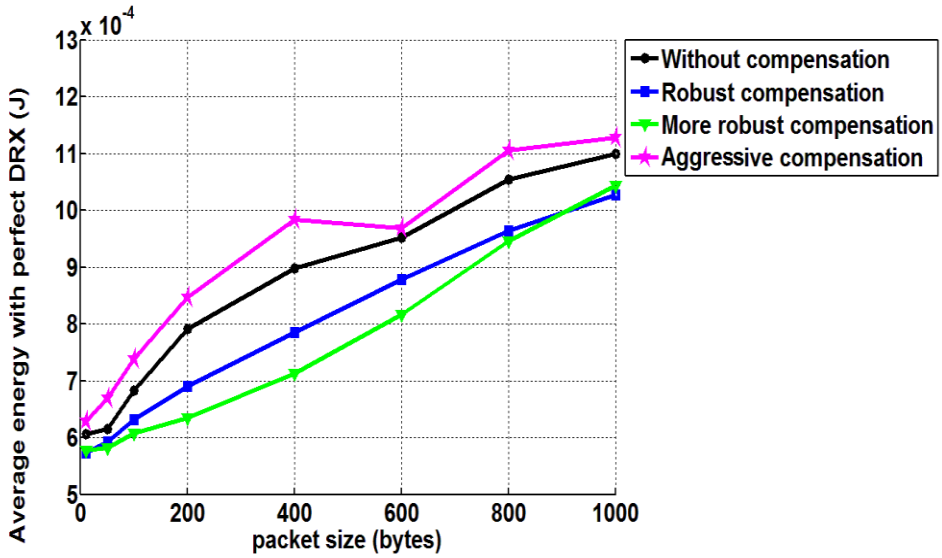

Fig. 51. Average percentile device energy consumption with perfect DRX

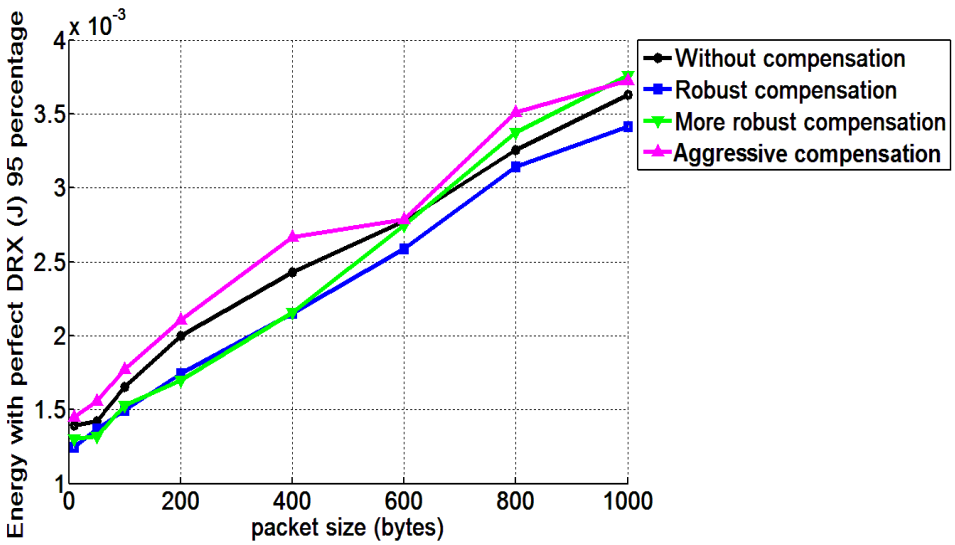

Fig. 52. 95th percentile device energy consumption with perfect DRX

4.2.6 Dynamic MCS design Case 3

The average device energy consumption per UE without DRX, 95th percentile device energy consumption without DRX, average device energy consumption with perfect DRX and 95th percentile device energy consumption with perfect DRX are shown in Figs. 53, 54, 55 and 56, respectively. As opposed to Case 1, the robust scheme is consistently better than the more robust scheme.

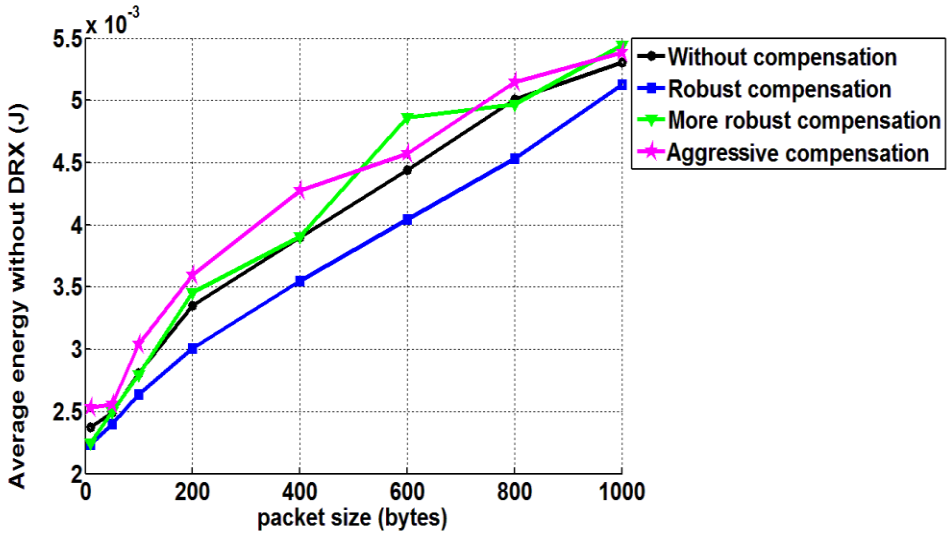

Fig. 53. Average device energy consumption without DRX

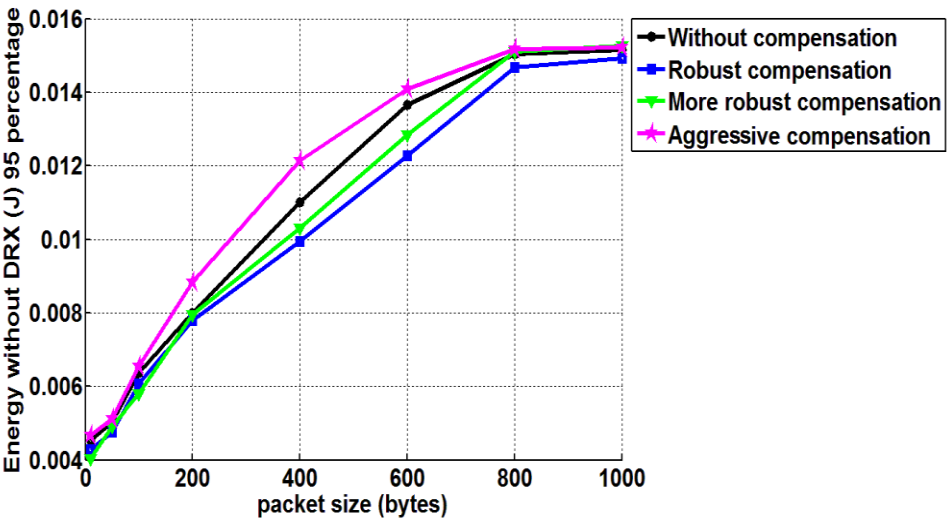

Fig. 54. 95th percentile device energy consumption without DRX

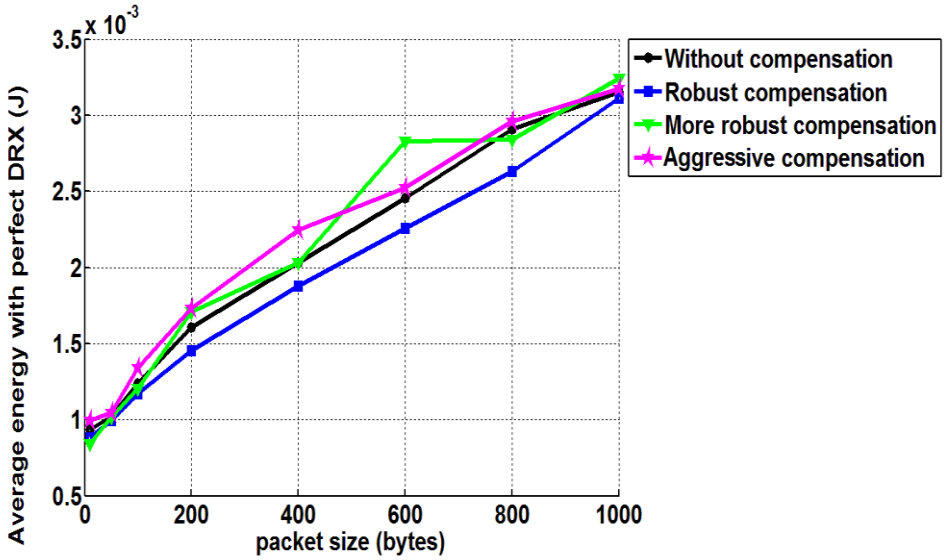

Fig. 55. Average percentile device energy consumption with perfect DRX

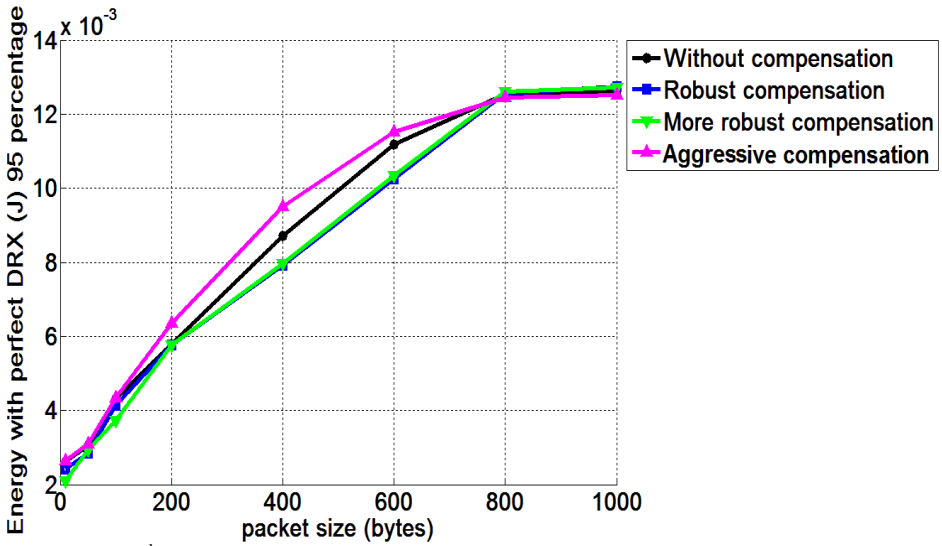

Fig. 56. 95th percentile device energy consumption with perfect DRX

4.2.7 Outer loop MCS design Case 1

The average device energy consumption per UE without DRX, 95th percentile device energy consumption without DRX, average device energy consumption with perfect DRX and 95th percentile device energy consumption with perfect DRX are shown in Figs. 57, 58, 59 and 60, respectively. It could be seen that the setting with 1 MSG3 attempt target provides more a robust performance with respect to energy consumption.

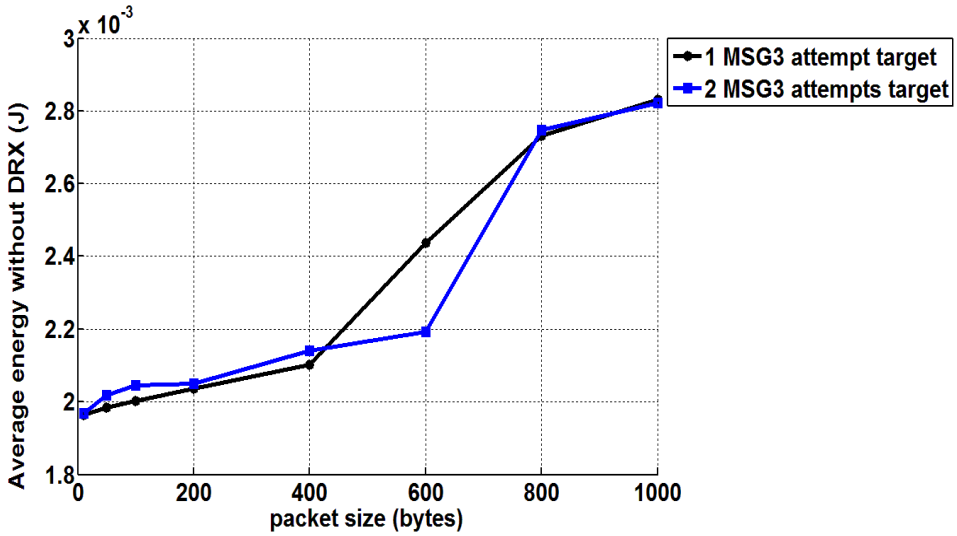

Fig. 57. Average device energy consumption without DRX

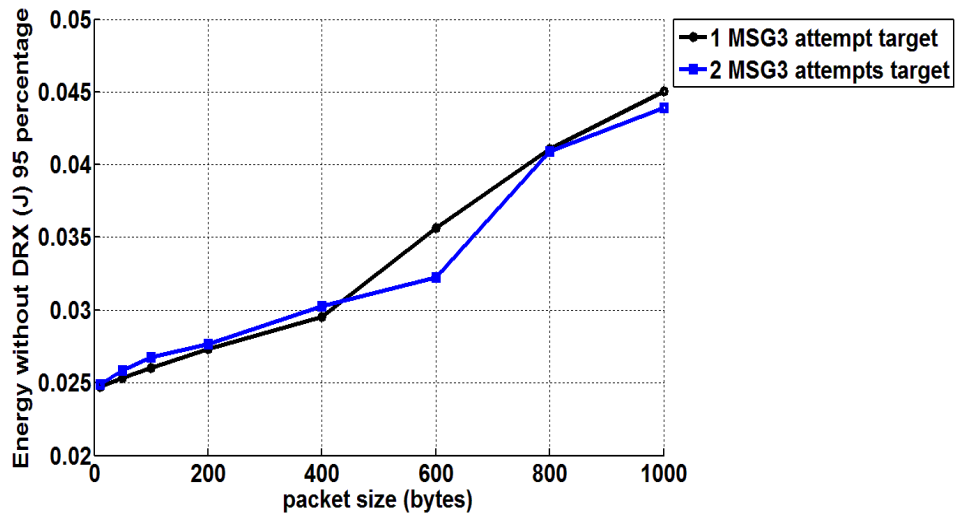

Fig. 58. 95th percentile device energy consumption without DRX

Moreover, similar trends in energy consumption for the two target settings are seen both with and without DRX.

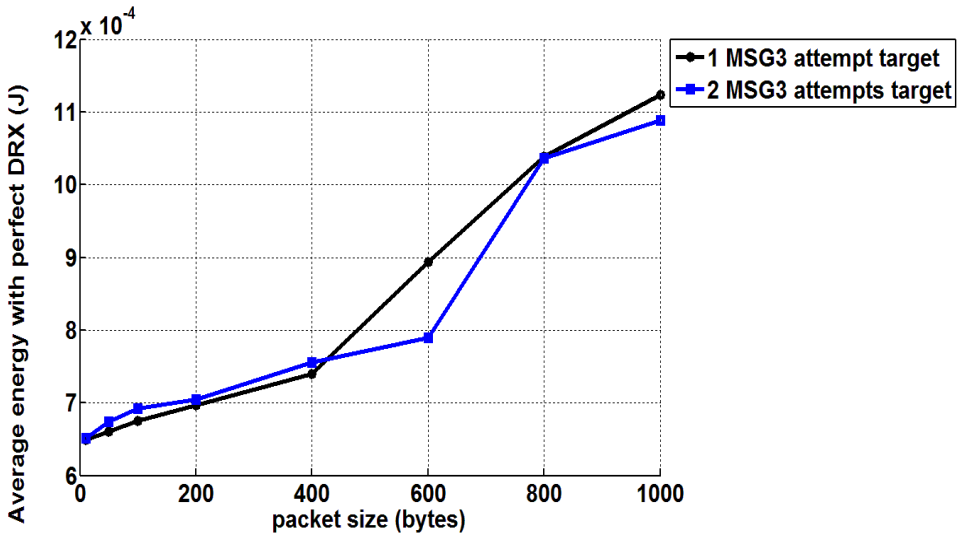

Fig. 59. Average percentile device energy consumption with perfect DRX

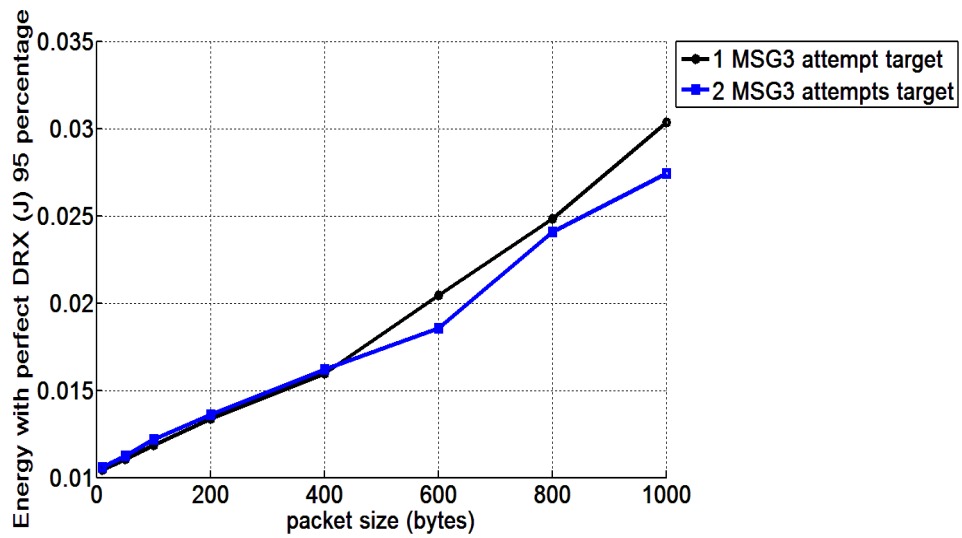

Fig. 60. 95th percentile device energy consumption with perfect DRX

4.2.8 Outer loop MCS design Case 3

The average device energy consumption per UE without DRX, 95th percentile device energy consumption without DRX, average device energy consumption with perfect DRX and 95th percentile device energy consumption with perfect DRX are shown in Figs. 61, 62, 63 and 64, respectively. It could be seen that larger packet sizes favor the setting with 2 MSG3 attempts target, as opposed to 1 MSG3 attempt target for smaller packet sizes. The crossover points occur near the packet size of 500 bytes.

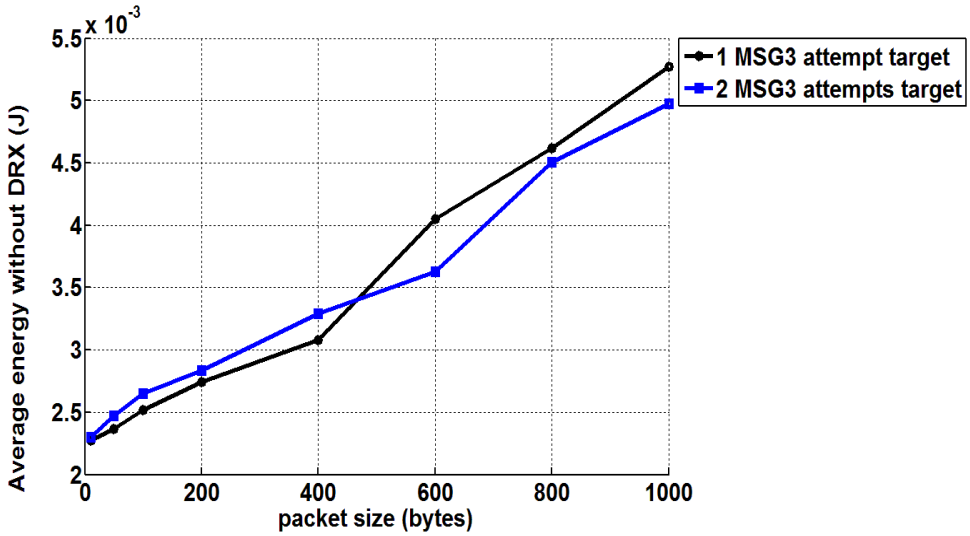

Fig. 61. Average device energy consumption without DRX

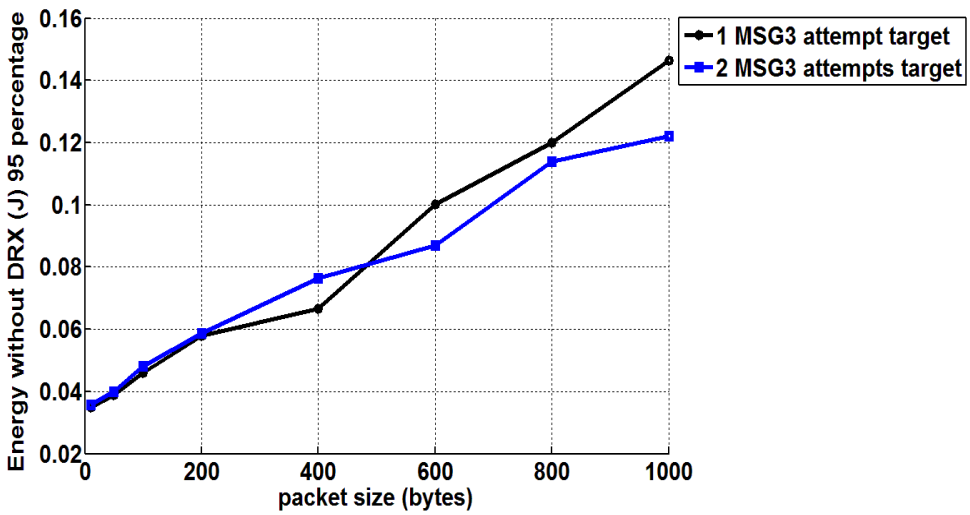

Fig. 62. 95th percentile device energy consumption without DRX

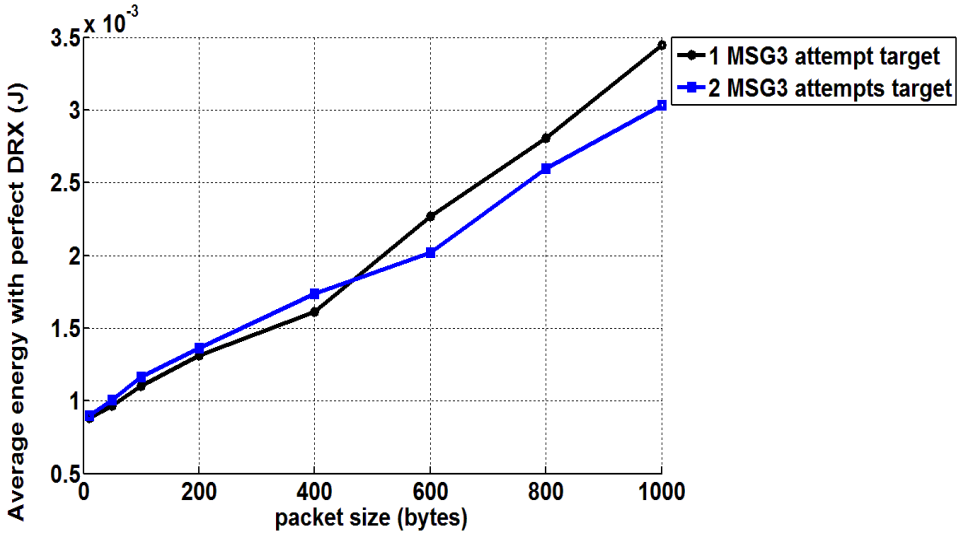

Fig. 63. Average percentile device energy consumption with perfect DRX

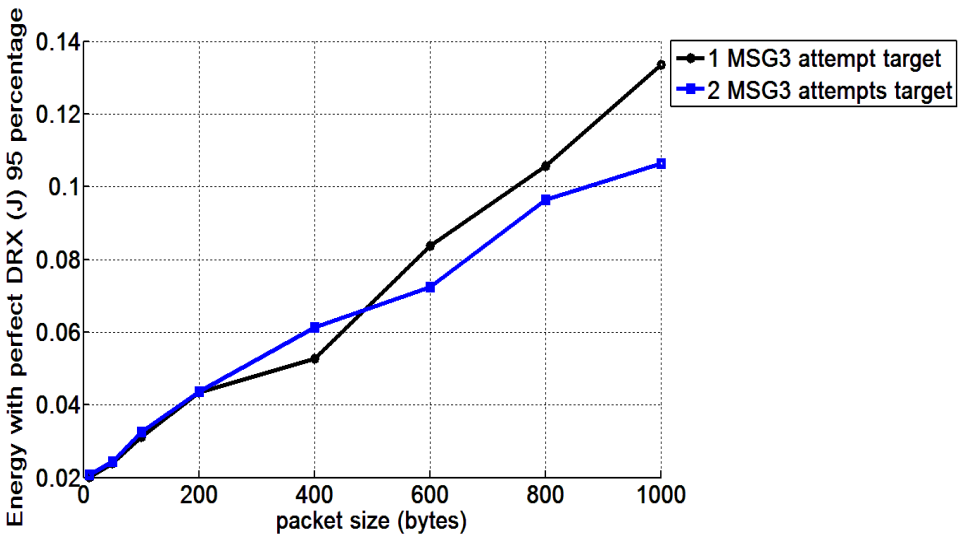

Fig. 64. 95th percentile device energy consumption with perfect DRX

4.2.9 Data transfer buffer estimation Case 1

The average device energy consumption per UE without DRX, 95th percentile device energy consumption without DRX, average device energy consumption with perfect DRX and 95th percentile device energy consumption with perfect DRX are shown in Figs. 65, 66, 67 and 68, respectively. The results show that there is potentially better performance on energy consumption under the designs with signaling reduction.

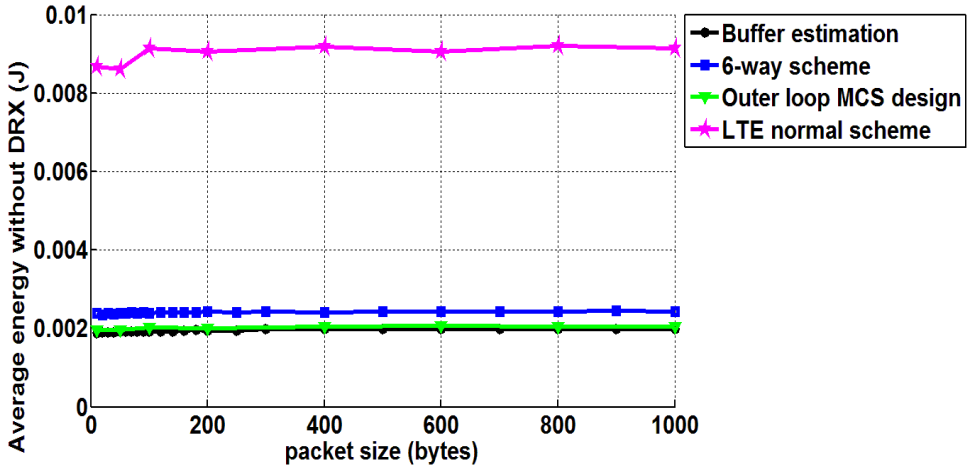

Fig. 65. Average device energy consumption without DRX

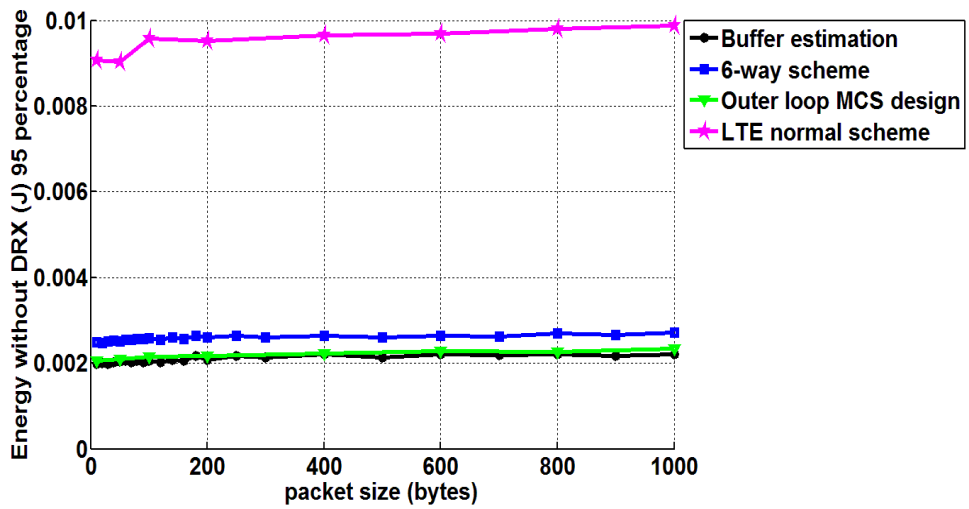

Fig. 66. 95th percentile device energy consumption without DRX

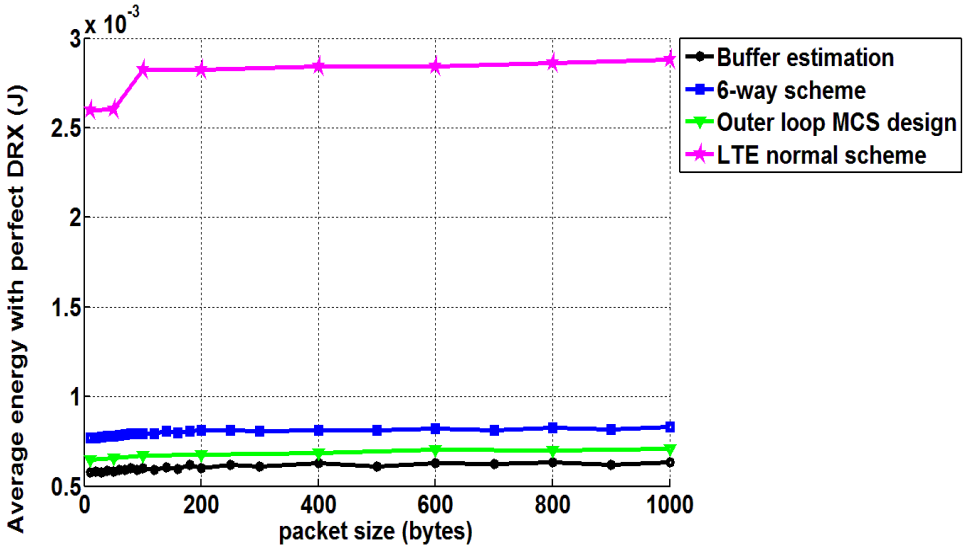

Fig. 67. Average percentile device energy consumption with perfect DRX

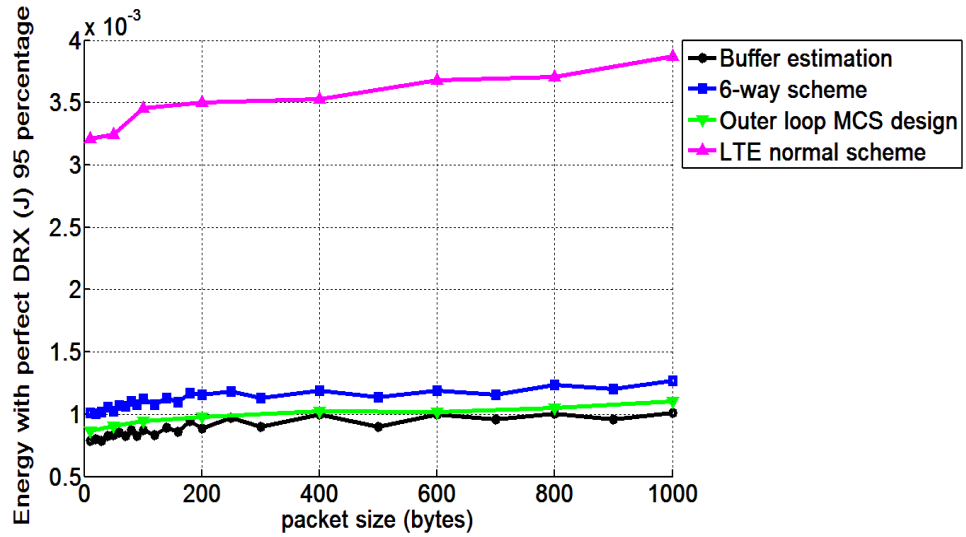

Fig. 68. 95th percentile device energy consumption with perfect DRX

4.2.10 Data transfer buffer estimation Case 3

The average device energy consumption per UE without DRX, 95th percentile device energy consumption without DRX, average device energy consumption with perfect DRX and 95th percentile device energy consumption with perfect DRX are shown in Figs. 69, 70, 71, and 72, respectively. Same conclusions as in Case 1 can be reached from these figures

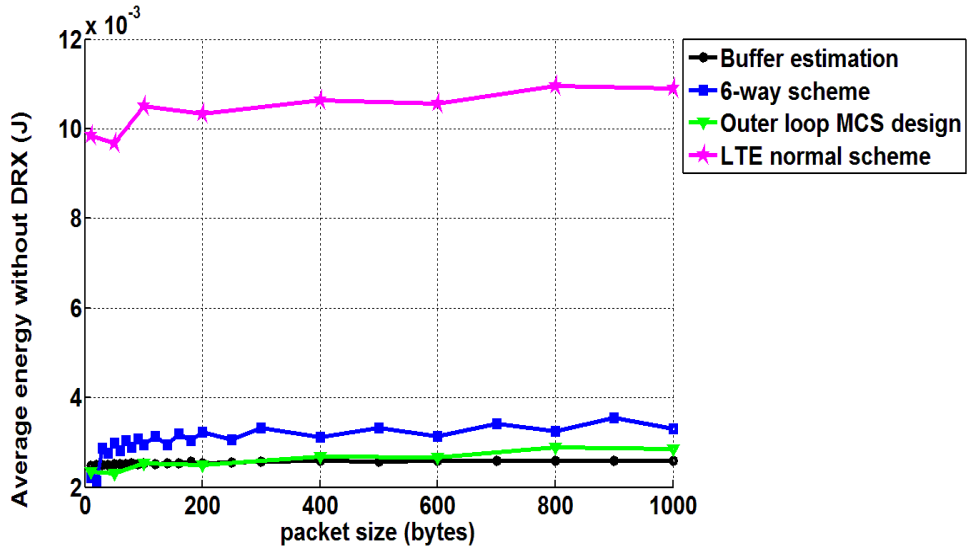

Fig. 69. Average device energy consumption without DRX

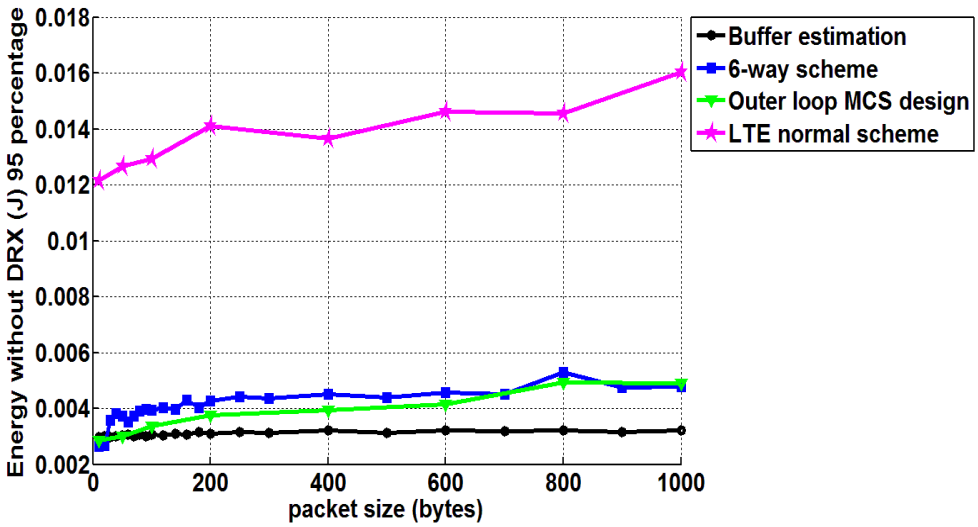

Fig. 70. 95th percentile device energy consumption without DRX

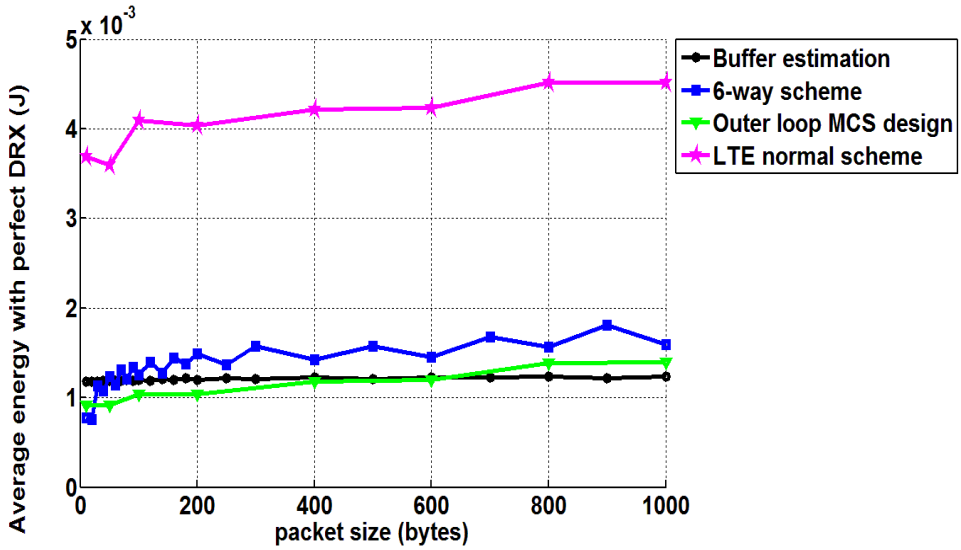

Fig. 71. Average percentile device energy consumption with perfect DRX

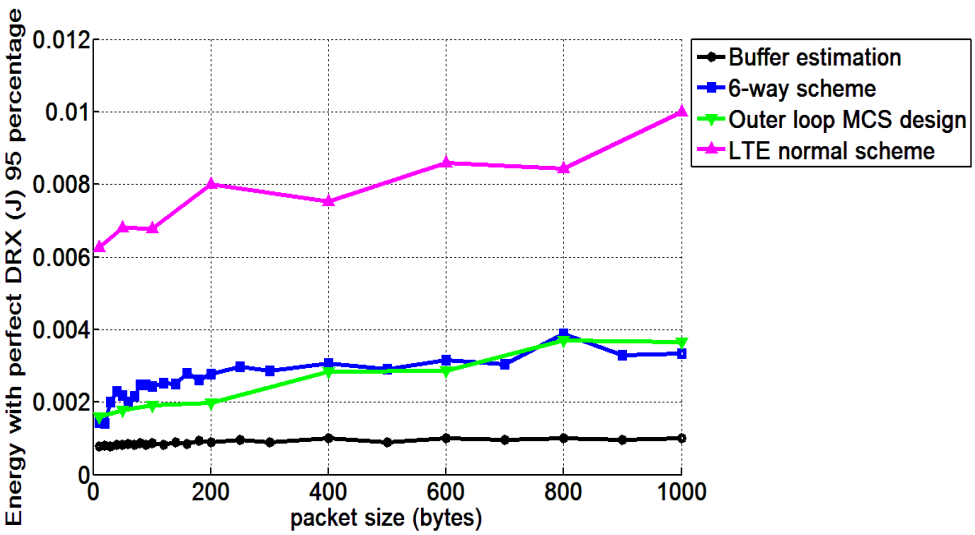

Fig. 72. 95th percentile device energy consumption with perfect DRX

4.3 Failure Users

The failure user performance measurement is shown with the failure rate of the network. It could be seen that with improper settings of parameters specific to the design, there could be much more failure users in the network. There are much more failure users in some cases when the simulations run in the 3GPP Case 3 radio environment than that in 3GPP Case 1 because the cell size in Case 1 is much smaller than that in case 3.

Note that the y axes differ between different designs because the plots are zoomed in on the relevant parts for each design case.

4.3.1 Normal scheme without release signaling Case 1

The failure rate of the network is shown in Fig. 73.

It could be seen the design could have good performance on failure rate even though there is signaling reduction. This is because the simple signaling reduction has no negative effects on link adaptation.

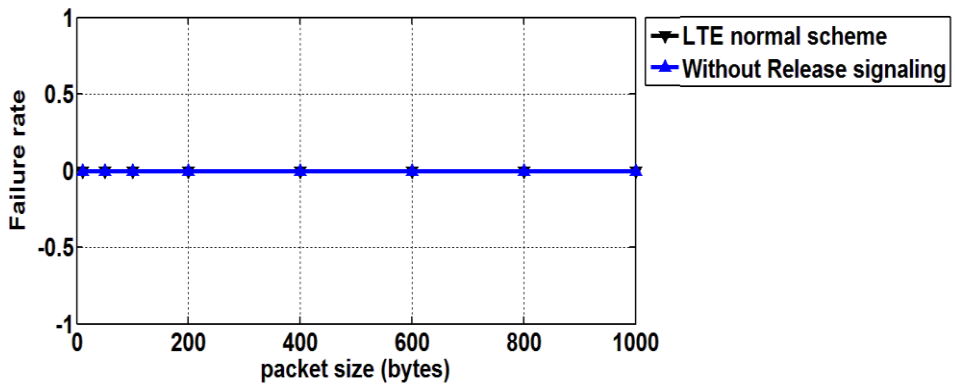

Fig. 73. Failure rate of network

4.3.2 Normal scheme without release signaling Case 3

The failure rate of the network is shown in Fig. 74.

It could be seen that even in Case 3 there could be good performance on failure rate with perfect link adaptation.

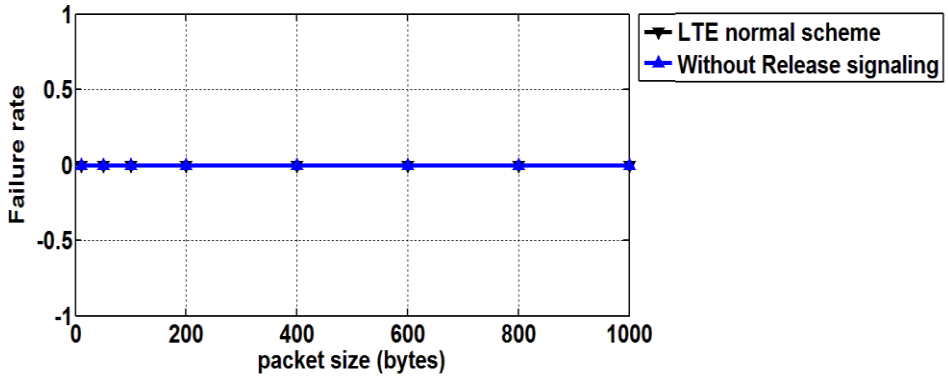

Fig. 74. Failure rate of network

4.3.3 Static MCS design Case 1

The failure rate of the network is shown in Fig. 75.

It could be seen that there will be much more failure rate in the network when the most aggressive MCS value setting is used. It could be explained by that when the user is in a poor channel condition, for example a cell edge user, it will have packet loss if the most aggressive MCS value is assigned to it.

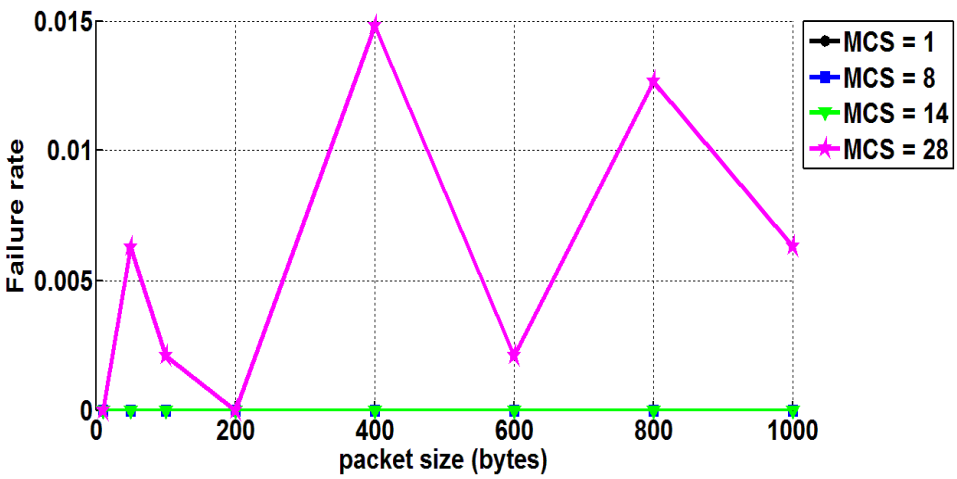

Fig. 75. Failure rate of network

4.3.4 Static MCS design Case 3

The failure rate of the network is shown in Fig. 76.

It could be seen that the failure rate in Case 3 is much higher than that in Case 1. The reason is that with a larger cell size, the loss of coverage could happen for the user in a poor channel condition, for example at the cell edge.

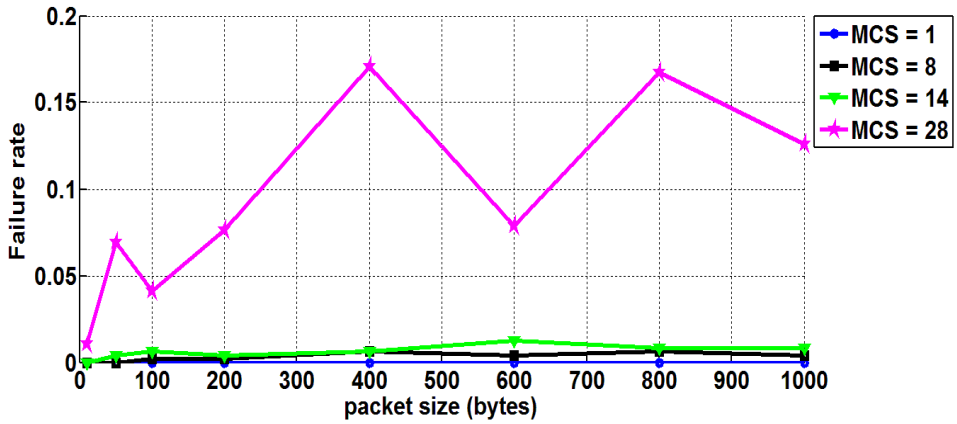

Fig. 76. Failure rate of network

4.3.5 Dynamic MCS design Case 1

The failure rate of the network is shown in Fig. 77.

It could be seen that with the robust compensation setting, the failure rate is significantly lower than that with the aggressive setting.

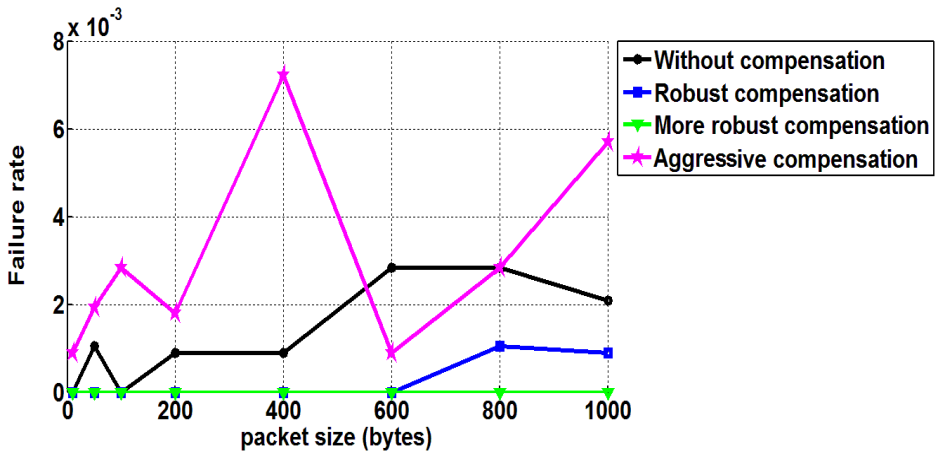

Fig. 77. Failure rate of network

4.3.6 Dynamic MCS design Case 3

The failure rate of the network is shown in Fig. 78.

It could be seen that the failure rate in Case 3 is higher than that in Case 1. This could be explained by that with a larger cell size, the loss of coverage could happen.

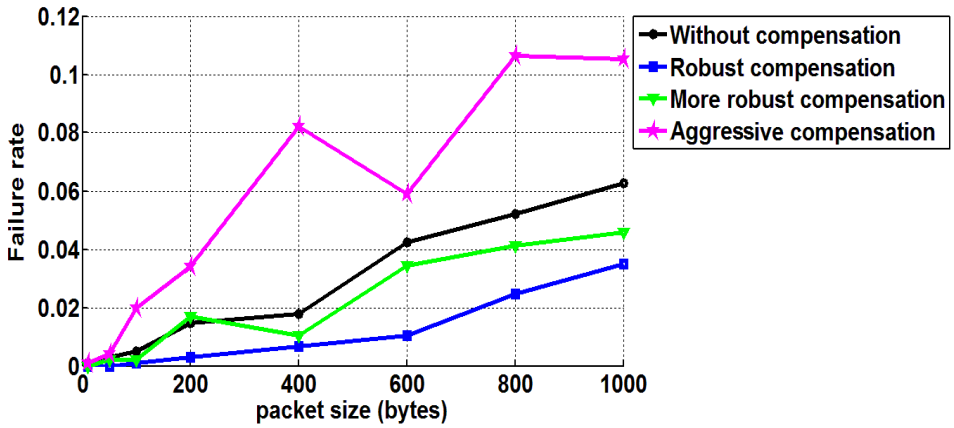

Fig. 78. Failure rate of network

4.3.7 Outer loop MCS design Case 1

The failure rate of the network is shown in Fig. 79.

It could be seen that with a proper setting, there could be zero failure rate of the network.

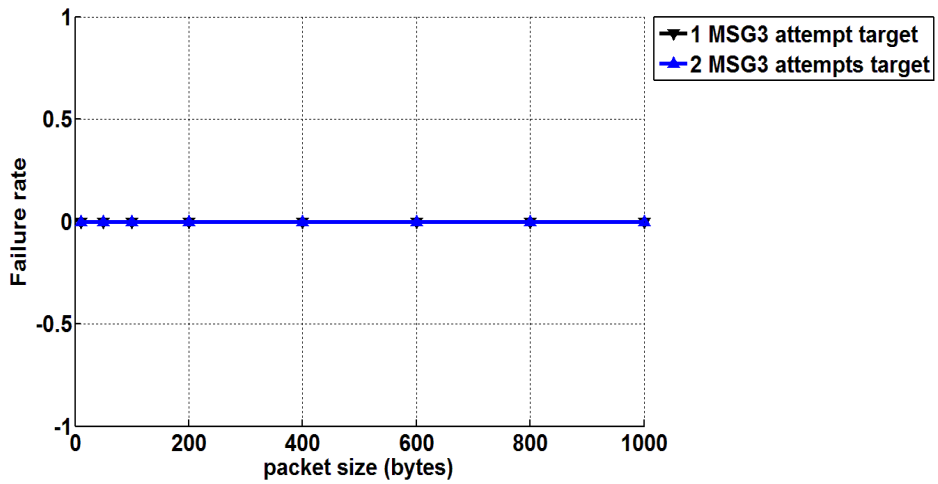

Fig. 79. Failure rate of network

4.3.8 Outer loop MCS design Case 3

The failure rate of the network is shown in Fig. 80.

It could be seen that even in Case 3, the performance is perfect if there is a proper setting for the design.

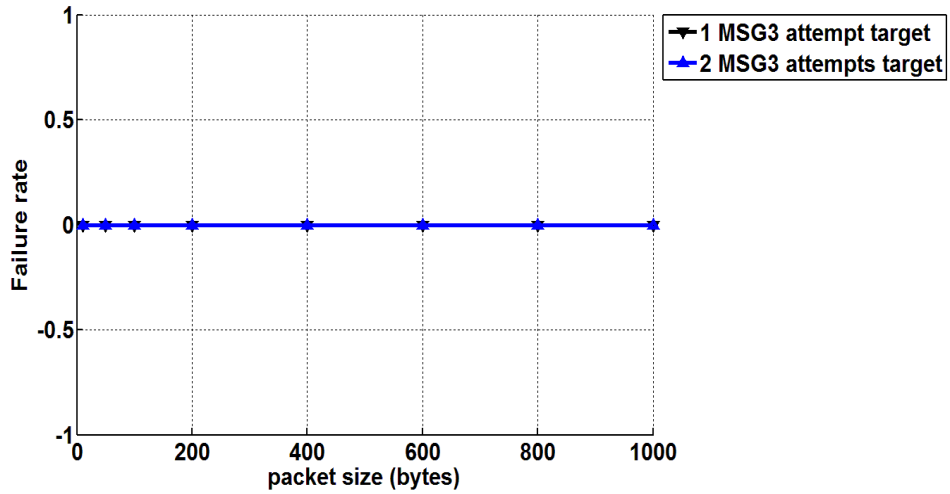

Fig. 80. Failure rate of network

4.3.9 Data transfer buffer estimation Case 1

The failure rate of the network is shown in Fig. 81.

It could be seen that with the proper settings of specifics parameters, the designs could have good performance on failure rate even though they are with signaling reduction.

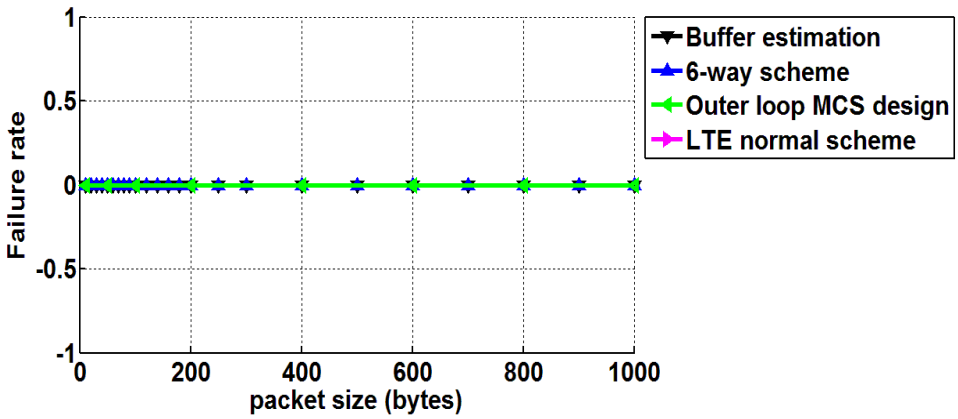

Fig. 81. Failure rate of network

4.3.10 Outer loop MCS design Case 3

The failure rate of the network is shown in Fig. 82.

It could be seen that even though the cell size in Case 3 is larger than that in Case 1, with the proper settings of specific parameters, there could be good performance on failure rate for the designs with signaling reduction.

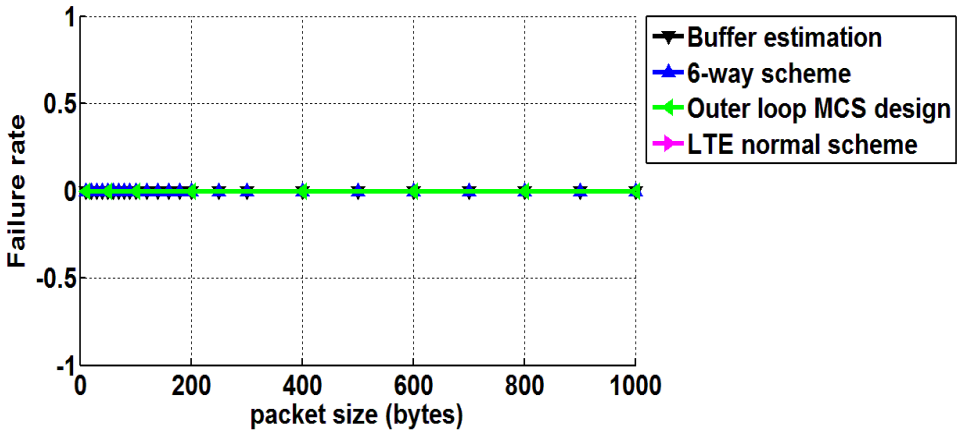

Fig. 82. Failure rate of network

4.4 Delay

The average delay per UE is shown in the following figures. It can be seen that with the proper settings of parameters specific to the design, the delay could be shorter. The results show a similar behavior as in the device energy consumption performance, with the exception that the more the device energy consumption is the larger the delay is. There is much more delay time when the simulations run in the 3GPP Case 3 radio environment than that in 3GPP Case 1 because the cell size in Case 1 is much smaller than that in Case 3.

Note that y axes differ between different designs because the plots are zoomed in on the relevant parts for each design case.

4.4.1 Normal scheme without release signaling Case 1

The average delay per UE is shown in Fig. 83.

It could be seen that with proper settings of parameters specific to the design, the delay could be shorter. The results show a similar behavior as in the device energy consumption performance, with the exception that the more the device energy consumption is the larger the delay is.

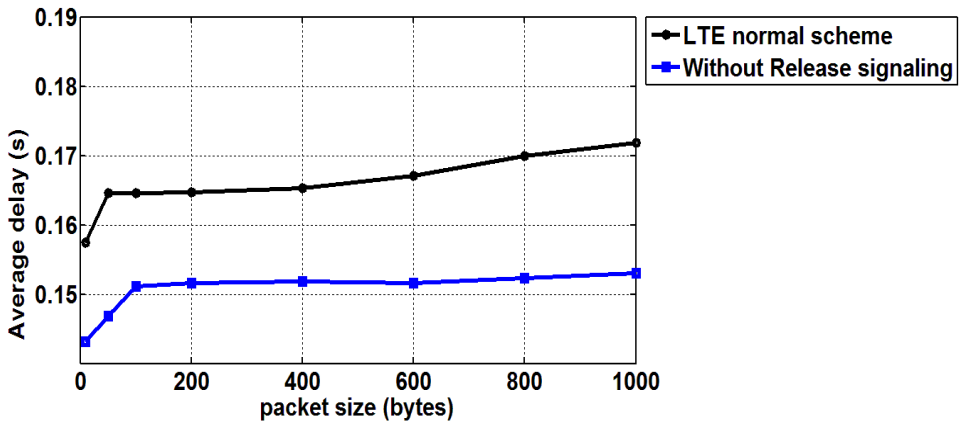

Fig. 83. Average delay

4.4.2 Normal scheme without release signaling Case 3

The average delay per UE is shown in Fig. 84. Similar trends as in Case 1 could be observed, except that the delay tends to increase more with packet size than in Case 1.

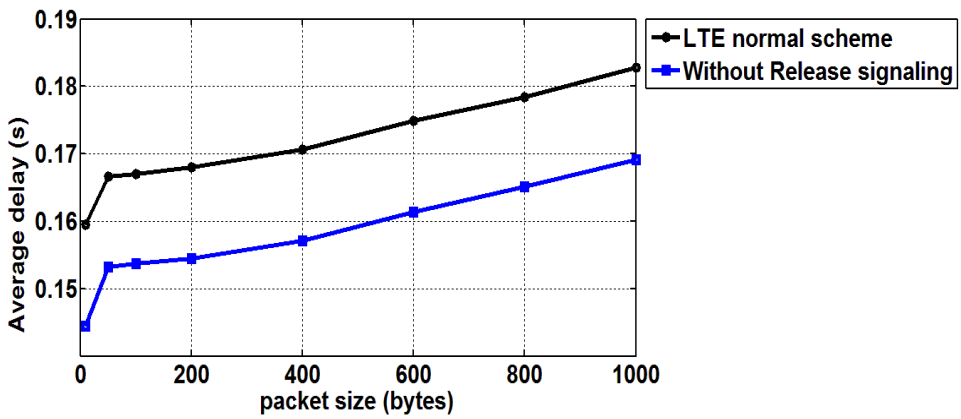

Fig. 84. Average delay

4.4.3 Static MCS design Case 1

The average delay per UE is shown in Fig. 85.

It could be seen that with proper settings of parameters specific to the design, which is MCS = 14, the delay could be shorter.

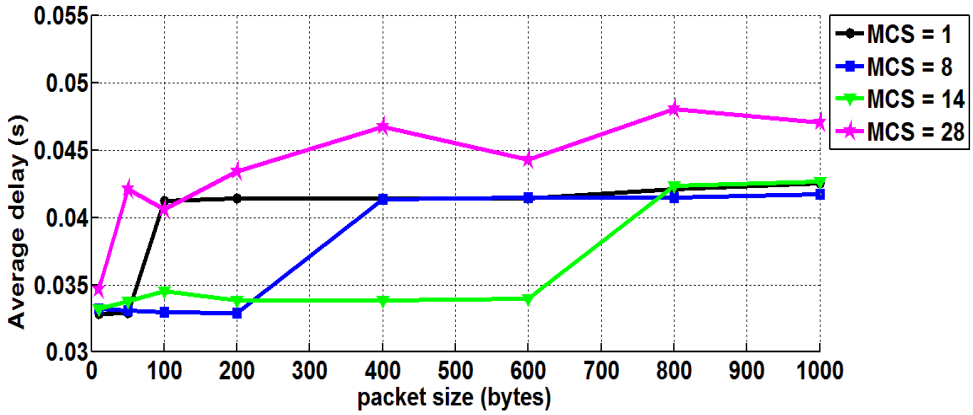

Fig. 85. Average delay

4.4.4 Static MCS design Case 3

The average delay per UE is shown in Fig. 86. In this case, the optimal performance seems to be achieved by a scheme between MCS = 8 and MCS = 14.

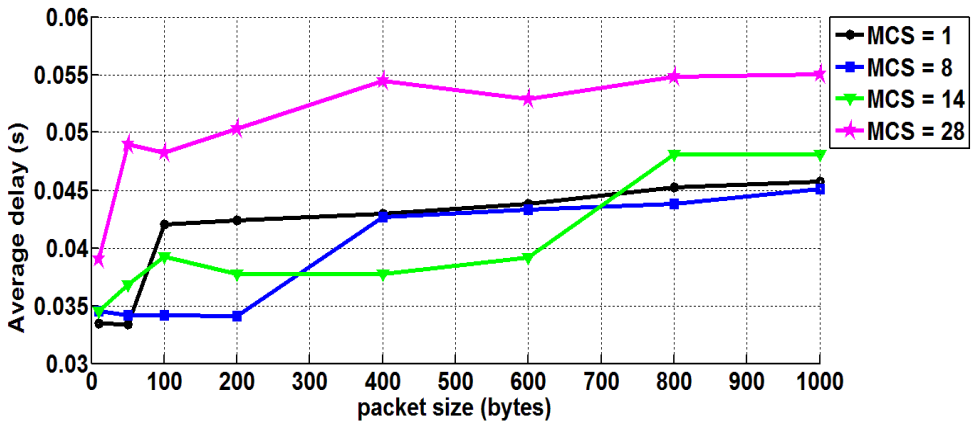

Fig. 86. Average delay

4.4.5 Dynamic MCS design Case 1

The average delay per UE is shown in Fig. 87.

In this design, the more robust compensation gives the lowest delay.

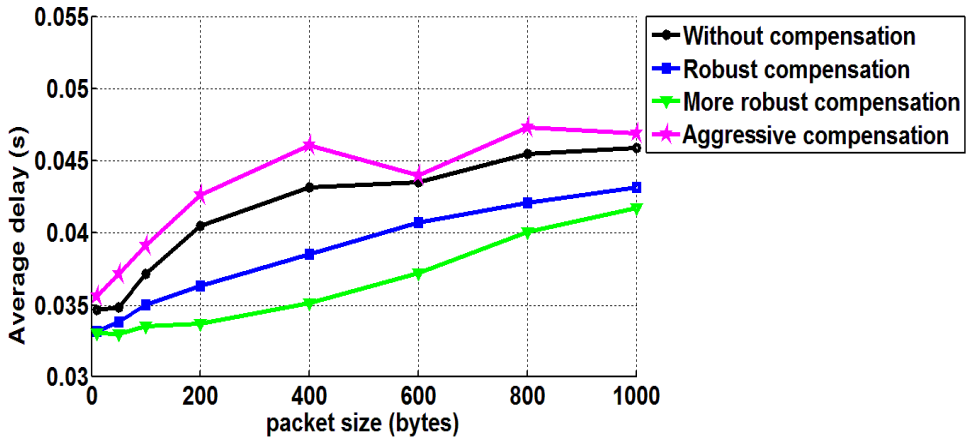

Fig. 87. Average delay

4.4.6 Dynamic MCS design Case 3

The average delay per UE is shown in Fig. 88.

As opposed to Case 1, the lowest delay here is achieved by the robust compensation.

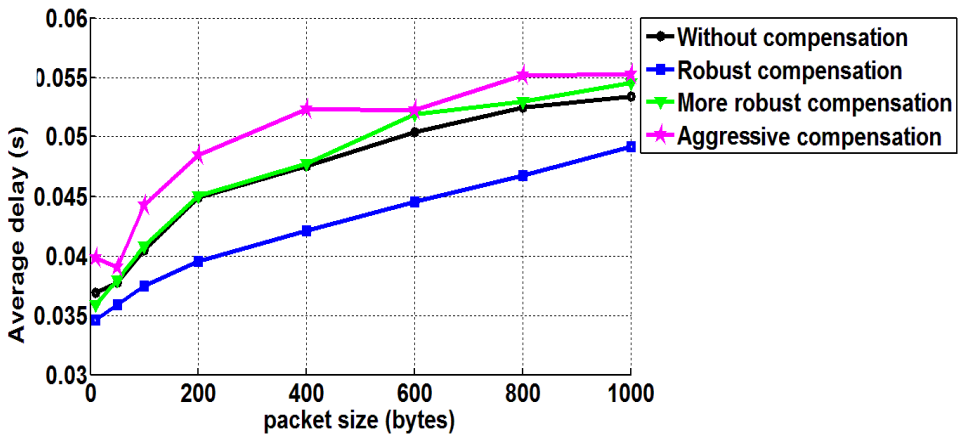

Fig. 88. Average delay

4.4.7 Outer loop MCS design Case 1

The average delay per UE is shown in Fig. 89. In this design, the 2 MSG3 attempts perform better in general except for moderate packet sizes.

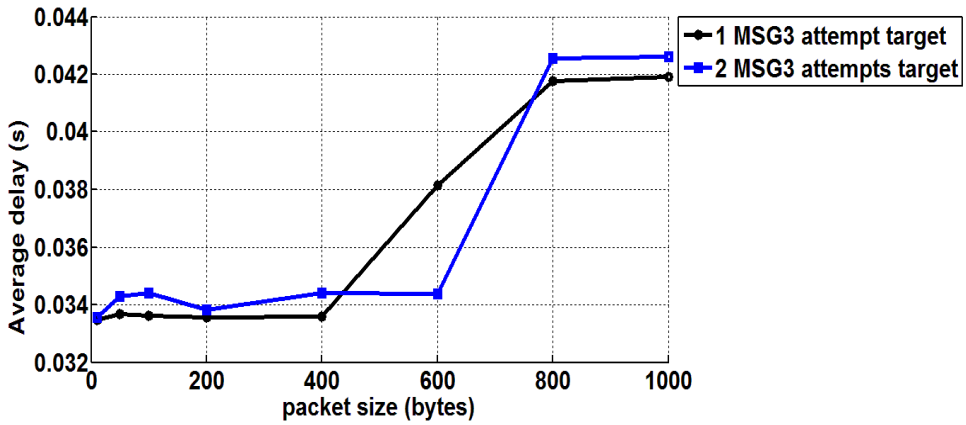

Fig. 89. Average delay

4.4.8 Outer loop MCS design Case 3

The average delay per UE is shown in Fig. 90. Similar trends as in Case 1 is observed.

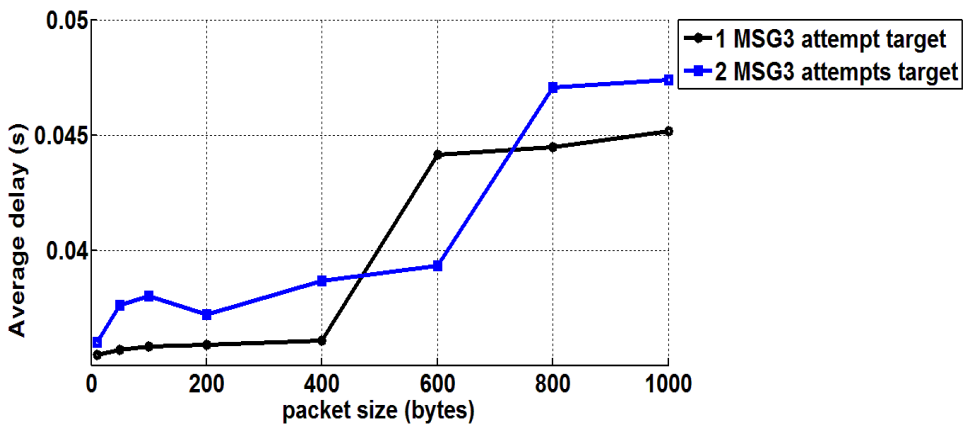

Fig. 90. Average delay

4.4.9 Data transfer buffer estimation design Case 1

The average delay per UE is shown in Fig. 91.

It could be seen that the designs with signaling reduction could have much better performance on delay.

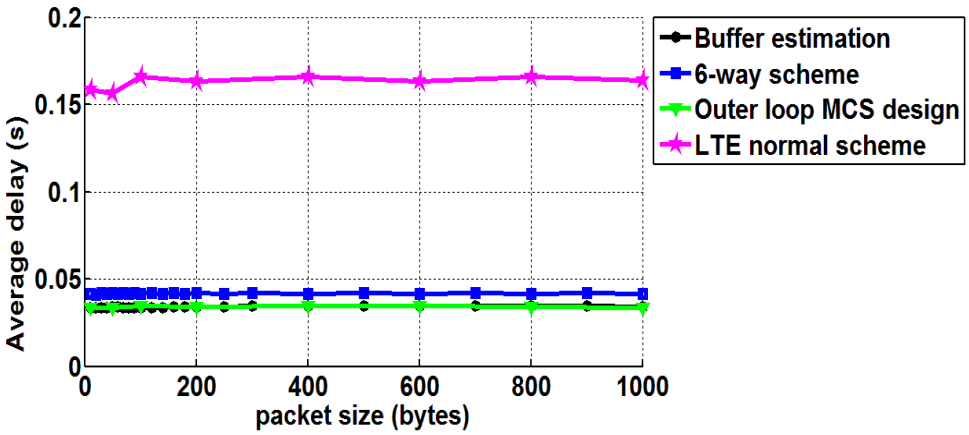

Fig. 91. Average delay

4.4.10 Data transfer buffer estimation design Case 3

The average delay per UE is shown in Fig. 92. Similar conclusions as in Case 1 could be reached.

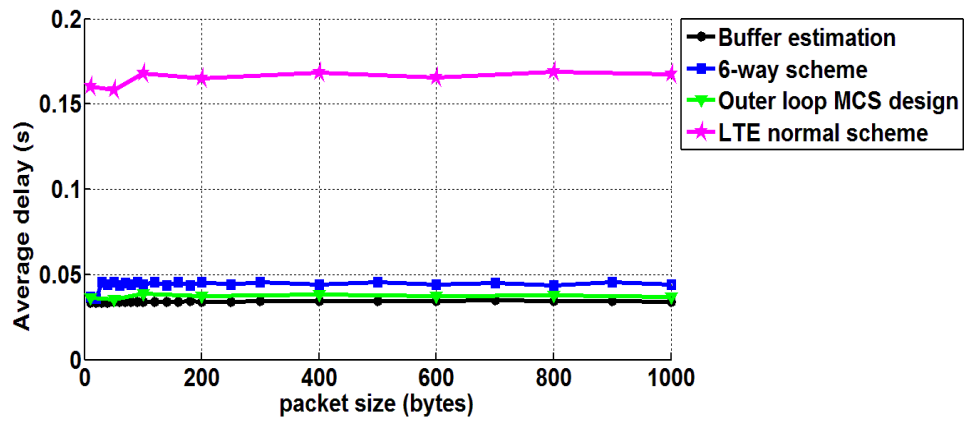

Fig. 92. Average delay

CHAPTER 5

5 Discussion

The results show that signaling reduction in the random access procedure with a proper link adaptation design is able to make the RRM efficient as long as the UL data transfer is small and infrequent. Referring to the simulation results, it is noted that the use of signaling reduction could cut radio resource utilization, device energy consumption and delay by more than 60 percent. This allows the designs with proper settings of specific parameters to have potentially good performance on such quality measures as radio resource utilization, device energy consumption, failure rate of network and delay.

An undesired effect is that as the settings of parameters specific to the designs are no longer proper, the measured performance will become poorer. For example, by setting the fixed MCS value equal to 1 in the static MCS design, the performance of the best users will be limited, since a user in a good channel condition is never assigned a higher MCS value than a user in a poor channel condition. On the other hand, by setting the MCS value to 28, a user in a poor channel condition (e.g. cell edge user) will experience a high failure rate, and the overall network performance could be even poorer than if the fixed MCS value of 1 was configured.

This effect could probably be somewhat mitigated by using dynamic design or outer loop design when the eNB could assign properly estimated MCS value or data transfer buffer size to the UEs. For example in dynamic MCS design, a user in a good channel condition, which is known by estimating the GINR value, could be assigned a higher MCS value than those of the users in poor channel conditions. This would be suitable for use in a real network since it could automatically adjust the settings of specific parameters. However, in the static MCS design, all users in the network have to use only one fixed MCS value.

Another observation is that the measured performance becomes worse when the UL data transfer buffer size is increased. As the packet size increases, the number of data transfer attempts will increase to complete the

transmission. Thus, the transmission may experience varied channel quality during the transmission of one packet, and in this case it could be difficult to have proper link adaptation in the signaling reduction scheme.

It could be seen from Chapter 4 that in delay performance, the results show a similar behavior as those of the device energy consumption performance, with the exception that the longer the delay is the more the device energy consumption is. This is because when the delay increases, the device has to generate more energy until the data transfer ends. It could also be observed that the performance differs under the same settings of parameter specific to the same design between the simulations run in the 3GPP Case 1 and 3GPP Case 3 radio environments. This is attributed to the significantly smaller inter-site distance (ISD) in Case 1 (500 meters) than that in Case 3 (1750 meters). Thus the channel condition differs a lot between these two cases.

It shall be noted that, regarding the PDSCH performance, there is no obvious difference in the same design with different settings of specific parameters, because the signaling reduction is mainly used to optimize small UL data transfers in this thesis. But in signaling reduction with no release signaling, it could be seen that there is less PDSCH usage than that in LTE normal scheme, since some downlink release signaling is removed in this case. It should also be noted that in some figures from the previous chapter, the curves are not very smooth. This is because each simulation is run with 20 different random seeds and it many more different random seeds or different settings of packet size may be needed to draw smoother curves.

CHAPTER 6

6 Conclusion

Signaling reduction in the random access procedure with efficient RRM could potentially give good performances, in terms of radio resource utilization, device energy consumption, failure rate of network and delay; as long as the UL data transfer packet size is small and infrequent. As could be concluded from the simulation results, the use of signaling reduction could cut radio resource utilization, device energy consumption and delay by more than 60 percent.

In case there is not enough signaling in the random access procedure to ensure successful UL data transfer, different link adaptation designs could use different approaches to handle this problem. For example, the dynamic MCS design uses the preamble sequence number to estimate the GINR value in order to assign a relevant MCS value to the UE; and the outer loop MCS design uses a statistical method to adjust the MCS value. Even in the data transfer buffer estimation design, not only the preamble sequence number is used to estimate the UL data transfer buffer size, but it also uses a statistical method to adjust the MCS value assigned to the UE.

Link adaptation design with signaling reduction in the random access procedure could work well in conjunction with proper settings of parameters specific to the design. Specifically, as verified with simulation results in this thesis, when the UL data transfers packets are small and infrequent, proper designs could offer better overall performance.

CHAPTER 7

7 Items for future study

This study mainly focused on small infrequent data transfer packet and efficient RRM with signaling reduction in the random access procedure. Some suggestions for future study are listed below:

- Traffic load: It may be interesting to investigate what benefits the different link adaptation designs can give under much heavier traffic loads.
- Mapping method: In this thesis, the data transfer buffer estimation design is combined with the outer loop MCS design, but not with the dynamic MCS design, because both the buffer estimation design and the dynamic MCS design make use of the preamble sequence number. However, it may also be interesting to study a new mapping method (in a new design) that could be used to combine the buffer estimation design and the dynamic MCS design.

References

[1] Erik. Dahlman, Stefan. Parkvall, Johan. Sköld and Per. Beming, *3G evolution HSPA and LTE for Mobile Broadband*, ACADAMIC PRESS, Publisher, first edition. ISBN 978-0-12-372533-2, 2007.

[2] 3GPP TS 36.201. E-UTRA; LTE physical layer; General description.

[3] 3GPP TS 36.133. E-UTRA; LTE Requirements for support of radio resource management.

[4] 3GPP TS 36.212. E-UTRA; Multiplexing and channel coding.

[5] 3GPP TS 36.211. E-UTRA; LTE Physical channels and modulation.

[6] 3GPP TS 36.213. E-UTRA; Physical layer procedures.

[7] 3GPP TS 36.321. E-UTRA; Medium Access Control (MAC) protocol specification.

[8] G. W. Miao, N. Himayat and G. Y. Li, "Energy-efficient link adaptation in frequency-selective channels," IEEE Trans. Commun., vol. 58, no. 2, pp.545-554, Feb. 2010.

[9] C.-C. Lee, J.-H. Yeh, and J.-C. Chen, "Impact of inactivity timer on energy consumption in WCDMA and cdma2000," in Wireless Telecommunications Symposium, 2004, May 2004, pp. 15 – 24.

[10] J. Wigard, T. Kolding, L. Dalsgaard, and C. Coletti, "On the user performance of lte ue power savings schemes with discontinuous reception in lte," in Communications Workshops, 2009. ICC Workshops 2009. IEEE International Conference on, june 2009, pp. 1-5.

[11] 3GPP TS 36.331. E-UTRA; Radio Resource Control (RRC); Protocol specification.

List of Acronyms

CQI	Channel Quality Indicator
C-RNTI	Cell Radio-Network Temporary Identifier
DL	Downlink
DRX	Discontinuous Reception
eNB	E-UTRAN NodeB
FTP	File Transfer Protocol
GINR	Gain-to-interference-and-noise ratio
ISD	inter-site distance
LTE	Long Term Evolution
MCS	Modulation and Coding Scheme
M2M	Machine to Machine
PDSCH	Physical Uplink Shared Channel
PSS	Primary Synchronization Signal
SSS	Secondary Synchronization Signal
PUSCH	Physical Downlink Shared Channel
QoS	Quality of Service
RA	Random Access
RACH	Random Access Channel
RB	Resource Block
RF	Radio Frequency
RRC	Radio Resource Control
RRM	Radio Resource Management
UL	Uplink
UE	User equipment

Appendix 1

A.1 Effects of the setting of parameters in the outer loop MCS design

In the outer loop MCS design, the setting of specific parameters concerns the number of MSG3 attempts target. When the statistic of the previous number of MSG3 attempts per UE is larger than the target setting of this parameter, the MCS value assigned to the UE will be decreased to guarantee that there should be fewer retransmissions. If the statistic is smaller than the target setting, the eNB will increase the MCS value assigned to the UE to make the transmission more aggressive. The purpose of this appendix is to study how the number of MSG3 attempts per UE varies in the network.

The average number of MSG3 attempts and 95th percentile number of MSG3 attempts are shown in Figs. 89, 90, 91 and 92, respectively. It could be seen from the figures that the setting of parameters specific to this design plays a role in controlling the number of MSG3 attempts in the network.

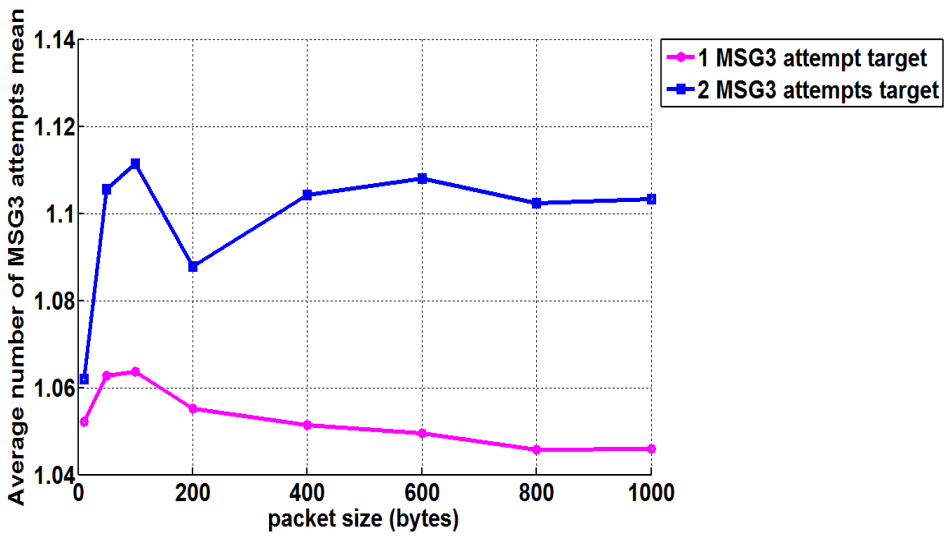

Fig. 93: Average number of MSG3 attempts

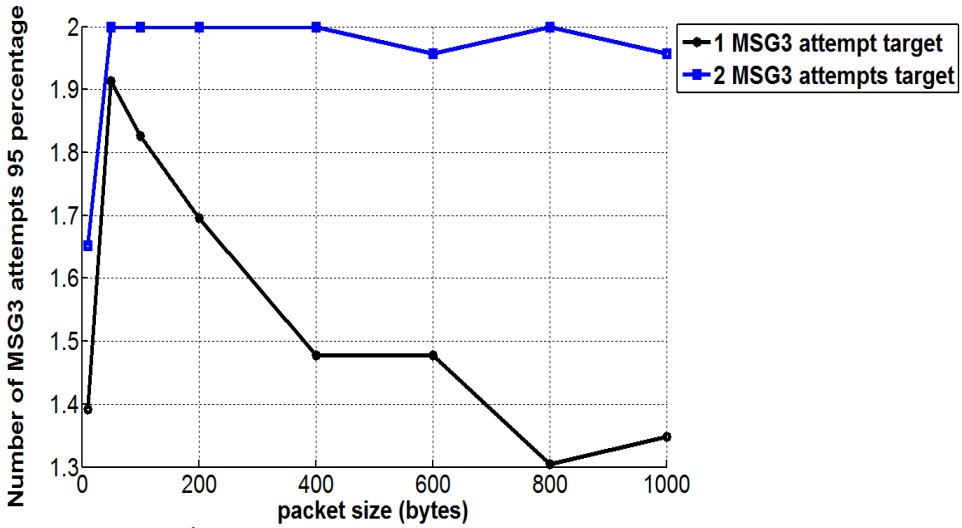

Fig. 94. 95th percentile number of MSG3 attempts in 3GPP Case 1

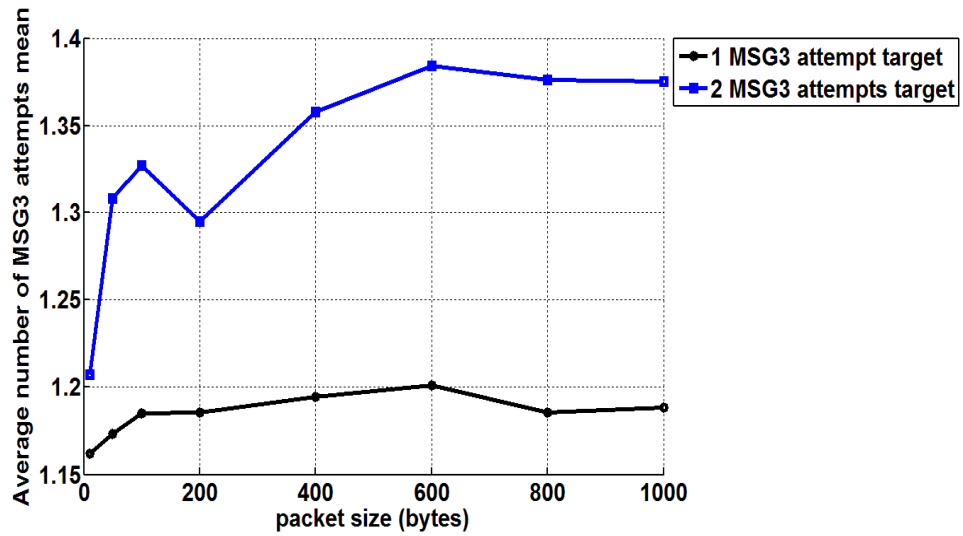

Fig. 95. Average number of MSG3 attempts in 3GPP Case 3

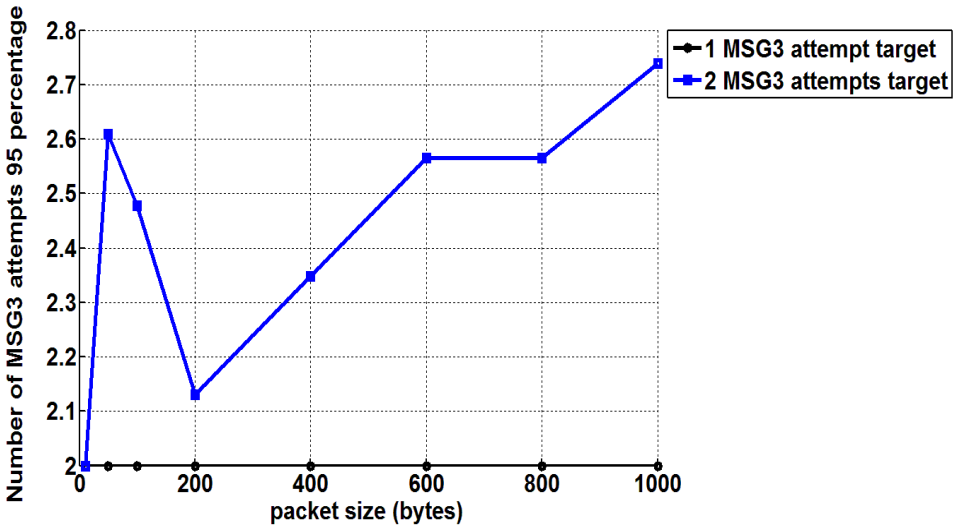

Fig. 96. Average number of MSG3 attempts in 3GPP Case 3

Appendix 2

A.2 Energy consumption of each component in the different designs

TABLE 10: DEVICE ENERGY CONSUMPTION OF EACH COMPONENT IN LTE NORMAL SCHEME WITHOUT RELEASE SIGNALING CASE 1

Each component	RX BB	RX RF	PA	TX RF	TX BB	Fine Clock	Total	Unit
LTE normal scheme with perfect DRX	0.6	0.5	0.7	0.2	0.01	1.7	3.1	mJ
LTE normal scheme without DRX	4.1	2.6	0.7	0.2	0.01	1.7	9.3	mJ
No Release signaling with perfect DRX	0.3	0.2	0.8	0.2	0.01	1.5	3	mJ
No Release signaling without DRX	3.8	2.4	0.8	0.2	0.01	1.5	8.6	mJ

TABLE 11: DEVICE ENERGY CONSUMPTION OF EACH COMPONENT IN LTE NORMAL SCHEME WITHOUT RELEASE SIGNALING CASE 3

Each component	RX BB	RX RF	PA	TX RF	TX BB	Fine Clock	Total	Unit
LTE normal scheme with perfect DRX	0.4	0.3	2.9	0.2	0.01	1.7	5.4	mJ

LTE normal scheme without DRX	4.3	2.7	2.9	0.2	0.01	1.7	11.8	mJ
No Release signaling with perfect DRX	0.3	0.3	2.9	0.2	0.01	1.6	5.3	mJ
No Release signaling without DRX	3.9	2.5	2.9	0.2	0.01	1.6	11.1	mJ

TABLE 12: DEVICE ENERGY CONSUMPTION OF EACH COMPONENT IN STATIC MCS DESIGN CASE 1

Each component	**RX BB**	**RX RF**	**PA**	**TX RF**	**TX BB**	**Fine Clock**	**Total**	**Unit**
MCS =1 with perfect DRX	0.1	0.1	0.4	0.2	0.01	0.4	1	mJ
MCS = 1 without DRX	1	0.6	0.4	0.2	0.01	0.4	2.6	mJ
MCS = 8 with perfect DRX	0.1	0.01	0.3	0.1	0.01	0.4	0.9	mJ
MCS = 8 without DRX	0.9	0.6	0.3	0.1	0.01	0.4	2.4	mJ
MCS = 14 with perfect DRX	0.1	0.06	0.3	0.1	0.01	0.4	0.8	mJ
MCS = 14 without DRX	0.9	0.6	0.3	0.1	0.01	0.4	2.2	mJ
MCS = 28 With perfect DRX	0.1	0.07	0.3	0.1	0.01	0.4	1	mJ
MCS = 28 without DRX	1.1	0.7	0.3	0.1	0.01	0.4	2.7	mJ

TABLE 13: DEVICE ENERGY CONSUMPTION OF EACH COMPONENT IN STATIC MCS DESIGN CASE 3

Each component	RX BB	RX RF	PA	TX RF	TX BB	Fine Clock	Total	Unit
MCS =1 with perfect DRX	0.1	0.1	2.3	0.2	0.01	0.4	3	mJ
MCS = 1 without DRX	1	0.6	2.3	0.2	0.01	0.4	4.6	mJ
MCS = 8 with perfect DRX	0.1	0.07	1.3	0.2	0.01	0.4	1.9	mJ
MCS = 8 without DRX	1	0.6	1.3	0.2	0.01	0.4	3.5	mJ
MCS = 14 with perfect DRX	0.1	0.07	1.2	0.1	0.01	0.4	1.8	mJ
MCS = 14 without DRX	1	0.6	1.2	0.1	0.01	0.4	3.4	mJ
MCS = 28 With perfect DRX	0.1	0.08	1.3	0.1	0.01	0.5	2	mJ
MCS = 28 without DRX	1.3	0.8	1.3	0.1	0.01	0.5	4	mJ

TABLE 14: DEVICE ENERGY CONSUMPTION OF EACH COMPONENT IN DYNAMIC MCS DESIGN CASE 1

Each component	RX BB	RX RF	PA	TX RF	TX BB	Fine Clock	Total	Unit
No compensation with perfect DRX	0.1	0.06	0.3	0.1	0.01	0.4	0.84	mJ
No compensation without DRX	1	0.6	0.3	0.1	0.01	0.4	2.4	mJ
Robust with perfect DRX	0.1	0.06	0.2	0.1	0.01	0.4	0.76	mJ

Robust without DRX	1	0.6	0.2	0.1	0.01	0.4	2.3	mJ
More robust with perfect DRX	0.1	0.06	0.2	0.1	0.01	0.4	0.74	mJ
More robust without DRX	0.9	0.6	0.2	0.1	0.01	0.4	2.2	mJ
Aggressive With perfect DRX	0.1	0.07	0.3	0.1	0.01	0.4	0.88	mJ
Aggressive without DRX	1.1	0.7	0.3	0.1	0.01	0.4	2.5	mJ

TABLE 15: DEVICE ENERGY CONSUMPTION OF EACH COMPONENT IN DYNAMIC MCS DESIGN CASE 3

Each component	**RX BB**	**RX RF**	**PA**	**TX RF**	**TX BB**	**Fine Clock**	**Total**	**Unit**
No compensation with perfect DRX	0.1	0.08	1.3	0.1	0.01	0.5	1.9	mJ
No compensation without DRX	1.1	0.7	1.3	0.1	0.01	0.5	3.7	mJ
Robust with perfect DRX	0.1	0.07	1.2	0.1	0.01	0.4	1.8	mJ
Robust without DRX	1	0.6	1.2	0.1	0.01	0.4	3.4	mJ
More robust with perfect DRX	0.1	0.08	1.3	0.1	0.01	0.5	2	mJ
More robust without DRX	1.1	0.7	1.3	0.1	0.01	0.5	3.8	mJ
Aggressive With perfect DRX	0.1	0.08	1.3	0.1	0.01	0.5	2	mJ
Aggressive without DRX	1.2	0.8	1.3	0.1	0.01	0.5	3.9	mJ

TABLE 16: DEVICE ENERGY CONSUMPTION OF EACH COMPONENT IN OUTER LOOP MCS DESIGN CASE 1

Each component	RX BB	RX RF	PA	TX RF	TX BB	Fine Clock	Total	Unit
1 MSG3 attempt with perfect DRX	0.1	0.06	0.3	0.1	0.01	0.4	0.81	mJ
1 MSG3 attempt without DRX	0.9	0.6	0.3	0.1	0.01	0.4	2.3	mJ
2 MSG3 attempts with perfect DRX	0.1	0.06	0.3	0.1	0.01	0.4	0.79	mJ
2 MSG3 attempts without DRX	0.9	0.6	0.3	0.1	0.01	0.4	2.2	mJ

TABLE 17: DEVICE ENERGY CONSUMPTION OF EACH COMPONENT IN OUTER LOOP MCS DESIGN CASE 3

Each component	RX BB	RX RF	PA	TX RF	TX BB	Fine Clock	Total	Unit
1 MSG3 attempt with perfect DRX	0.1	0.07	1.2	0.1	0.01	0.4	1.8	mJ
1 MSG3 attempt without DRX	1	0.6	1.2	0.7	0.01	0.4	3.4	mJ
2 MSG3 attempts with perfect DRX	0.1	0.07	1.1	0.1	0.01	0.4	1.7	mJ
2 MSG3 attempts without DRX	1	0.6	1.1	0.1	0.01	0.4	3.3	mJ

TABLE 18: DEVICE ENERGY CONSUMPTION OF EACH COMPONENT IN DATA TRANSFER BUFFER ESTIMATION DESIGN CASE 1

Each component	**RX BB**	**RX RF**	**PA**	**TX RF**	**TX BB**	**Fine Clock**	**Total**	**Unit**
Buffer estimation with perfect DRX	0.08	0.05	0.1	0.1	0.01	0.3	0.6	mJ
Buffer estimation without DRX	0.9	0.5	0.1	0.1	0.01	0.3	1.9	mJ

TABLE 19: DEVICE ENERGY CONSUMPTION OF EACH COMPONENT IN DATA TRANSFER BUFFER ESTIMATION DESIGN CASE 3

Each component	**RX BB**	**RX RF**	**PA**	**TX RF**	**TX BB**	**Fine Clock**	**Total**	**Unit**
Buffer estimation with perfect DRX	0.09	0.05	1	0.1	0.01	0.3	1.5	mJ
Buffer estimation without DRX	0.9	0.5	1	0.1	0.01	0.3	2.9	mJ